2008 CIG Numerical Modeling Workshop
Chemical Heterogeneity: Tracers and Entrainment

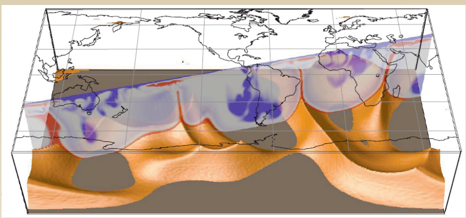

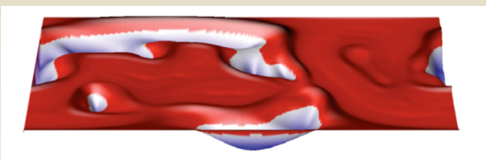

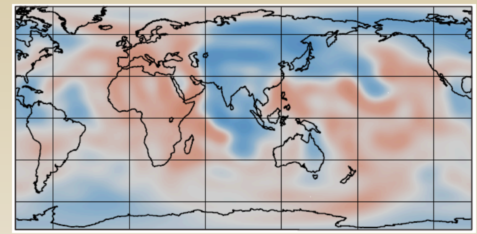

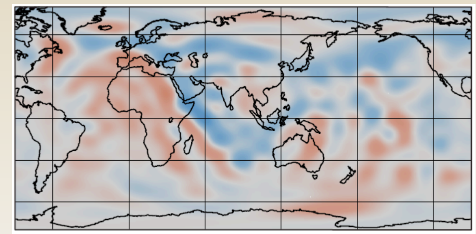

Allen K. McNamara

School of Earth and Space Exploration

Arizona State University

Includes research by Abigail Bull and Teresa Lassak.
Thanks to Thorsten Becker, Ed Garnero, Carolina Lithgow-Bertelloni, Sebastian Merkel, Jeroen Ritsema, Sebastian Rost, Lars Stixrude, Rudy Wenk, and Shijie Zhong

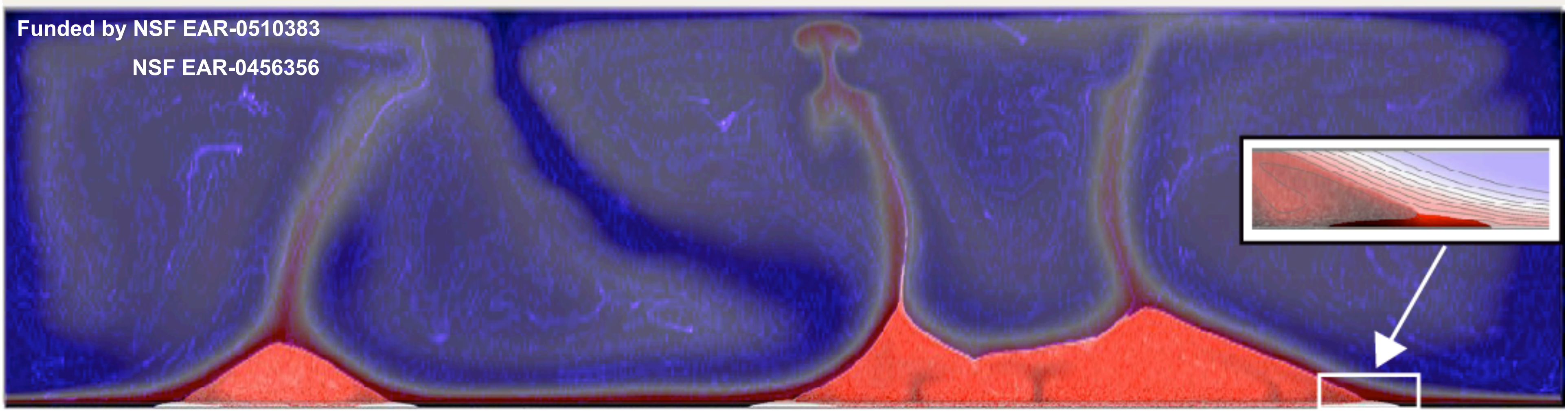

Funded by NSF EAR-0510383

NSF EAR-0456356

1. Common components of tracing in geodynamical codes
    - Comments about tracing in CitcomS
      (thermochemical extension released to CIG in 2007, thanks to Eh Tan)

2. Common uses for tracers, along with research examples
    - Deformation tracking
        - Example (providing an online resource for seismic anisotropy prediction)
    - Thermochemical convection
        - Example (small-scale ULVZ modeling)
    - Multiple rheologies
        - Example (lithospheric strength and crustal weakness)

3. Investigating large scale mantle convection using thermochemical convection
    - Modeling thermochemical piles and plume clusters
    - Investigating tomography as a constraint (Abigail Bull)
    - Investigating CMB topography as a constraint (Teresa Lassak)

Implementing tracers into a finite element code involves:

- storing relevant information with the tracer (e.g., advection quantities (for parallel), species information (composition, rheology, chemistry), history)
- finding which processor domain a tracer is currently in (for parallel)
- finding which element a tracer is currently in
- interpolating the velocity of the tracer, using velocities at element nodes
- advecting the tracer using a scheme that minimizes processing time, yet provides adequate compositional resolution.
- converting the distribution of Lagrangian tracers to compositional values on the mesh (e.g., absolute method, ratio method)

Its often convenient to have multiple tracer sets. Compositional tracers, rheological tracers, passive tracers, and deformation tracers can exist independently within the same calculation. This is made easy using structures in C. There is probably an equivalent in F90?

These components are relatively straightforward in most geodynamical convection codes that have element boundaries aligned with coordinate directions.

Non-standard aspects of tracer advection in CitcomS

1. Finding which element a tracer is in.

Use a finer “regular” mesh (e.g. van Keken and Ballentine (1998), van Keken and Zhong, 1999; McNamara et al. (2003))

2. Interpolation of tracer velocity

One way to do it is to transform coordinates using a gnomonic transformation.

User may define alternative methods!

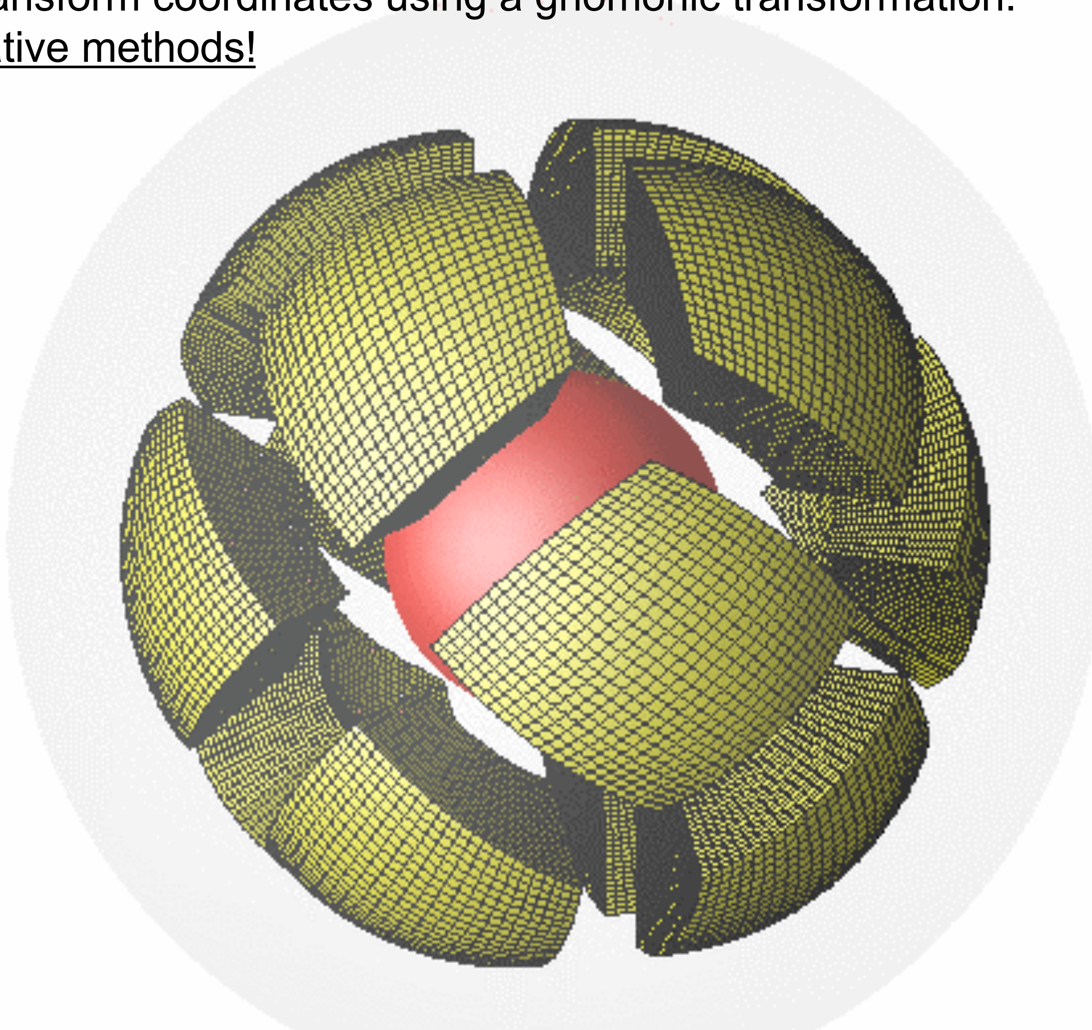

Elements are bounded by great circle planes.
Element boundaries are not related to coordinate system.

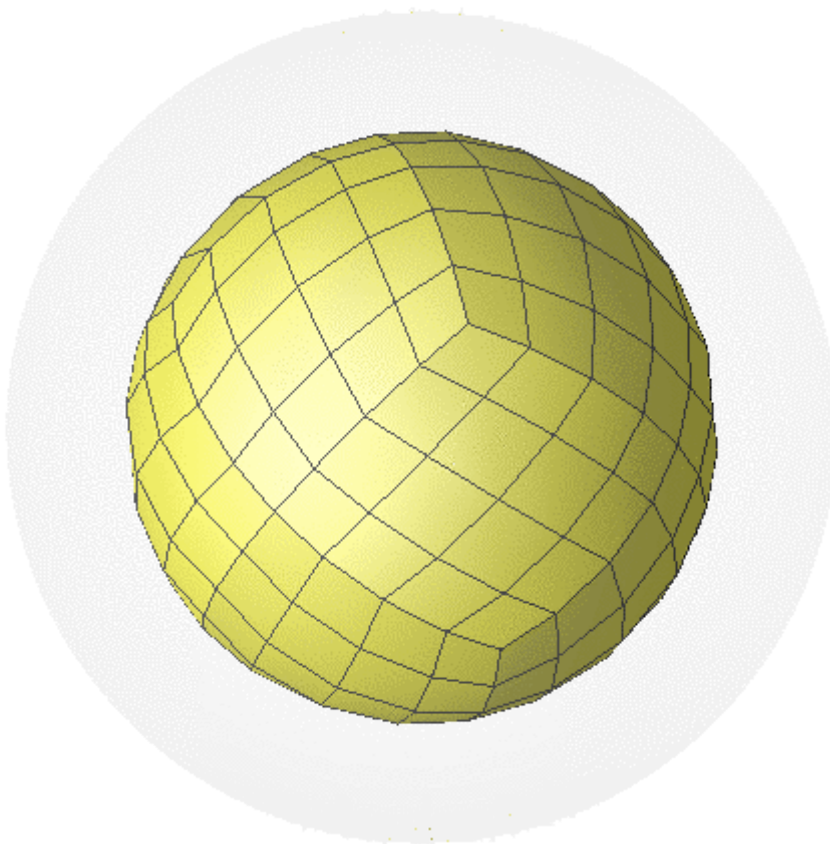

If the cross products of a boundary vector and a vector pointing to a tracer is in the positive r direction for all 4 boundaries, the tracer is in the element.

But this is slow.

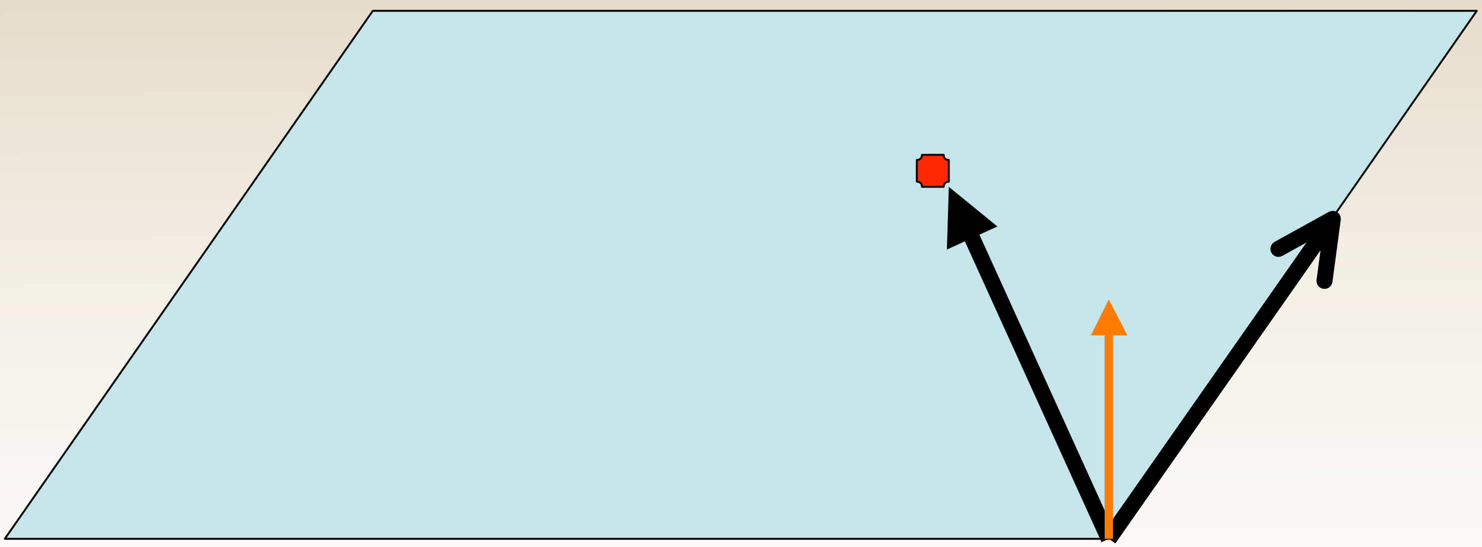

Superimpose a very fine regular grid which is aligned with the spherical coordinate system

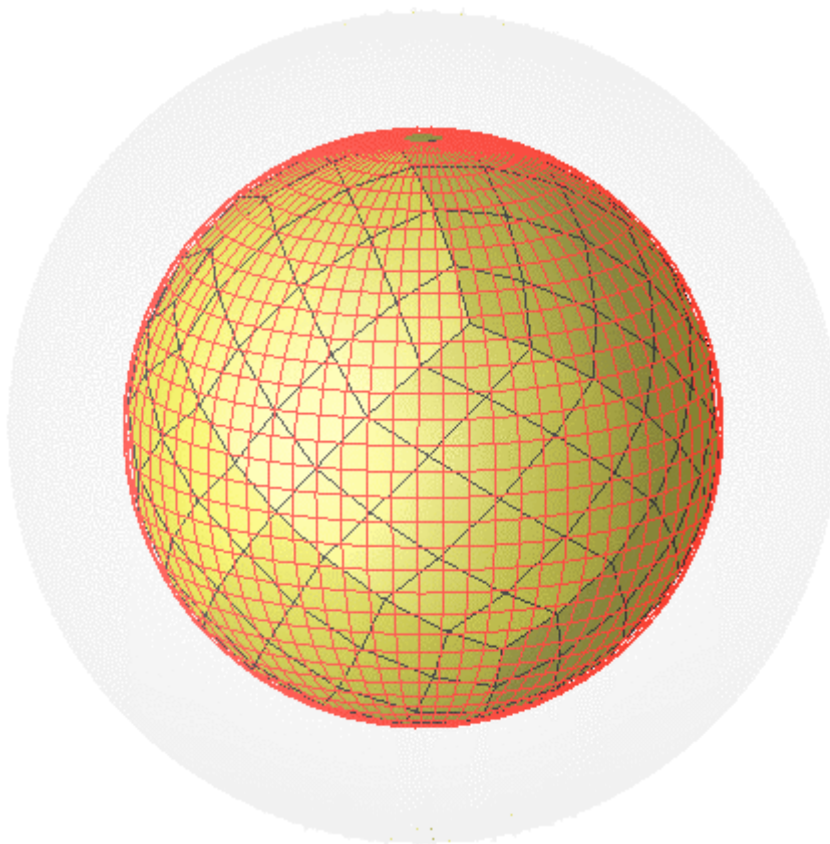

I find that a 0.1 x 0.1 degree regular mesh does a pretty good job for most calculations

Map the regular mesh to the real CitcomS mesh before the first timestep

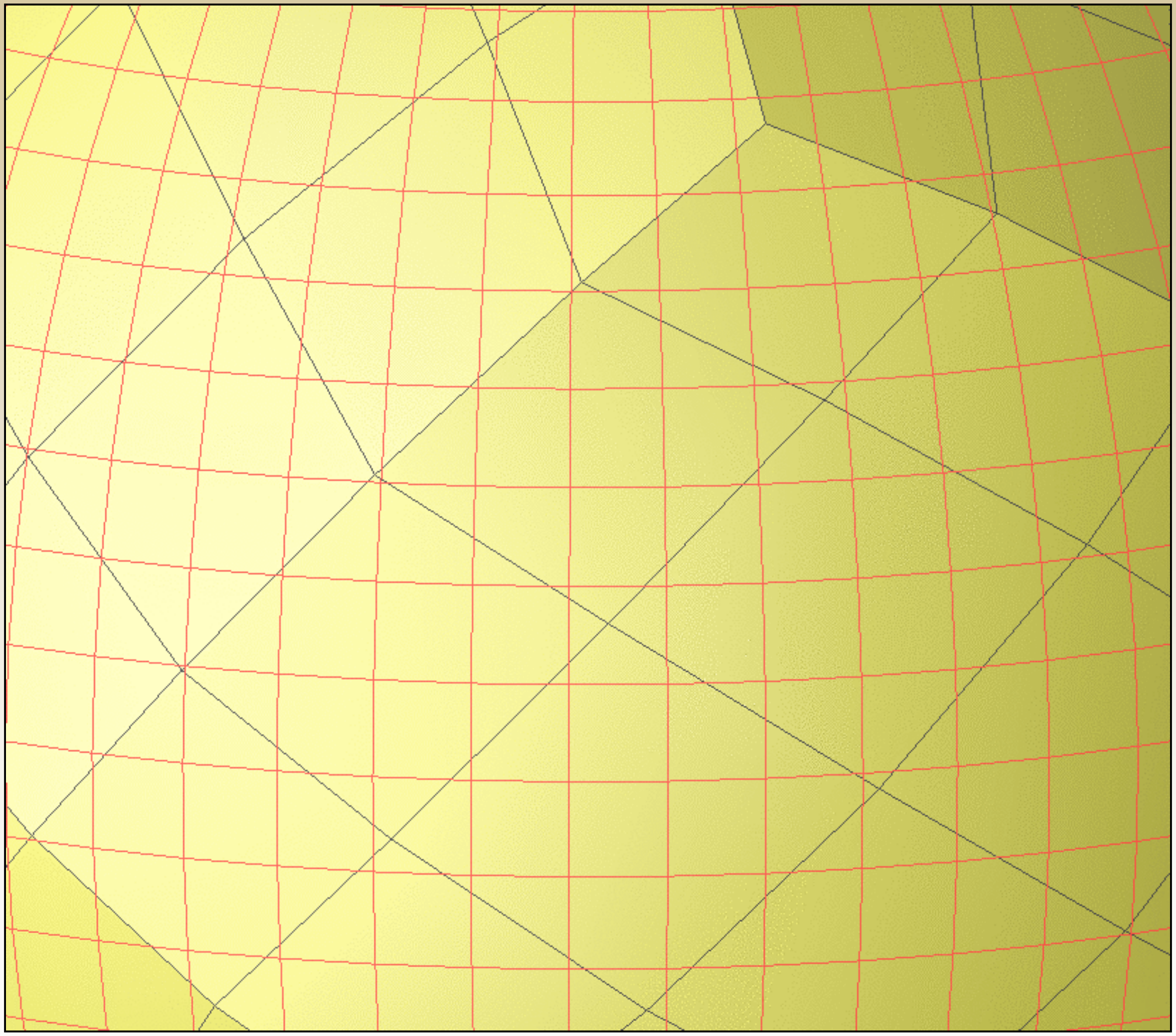

Map the regular mesh to the real CitcomS mesh before the first timestep

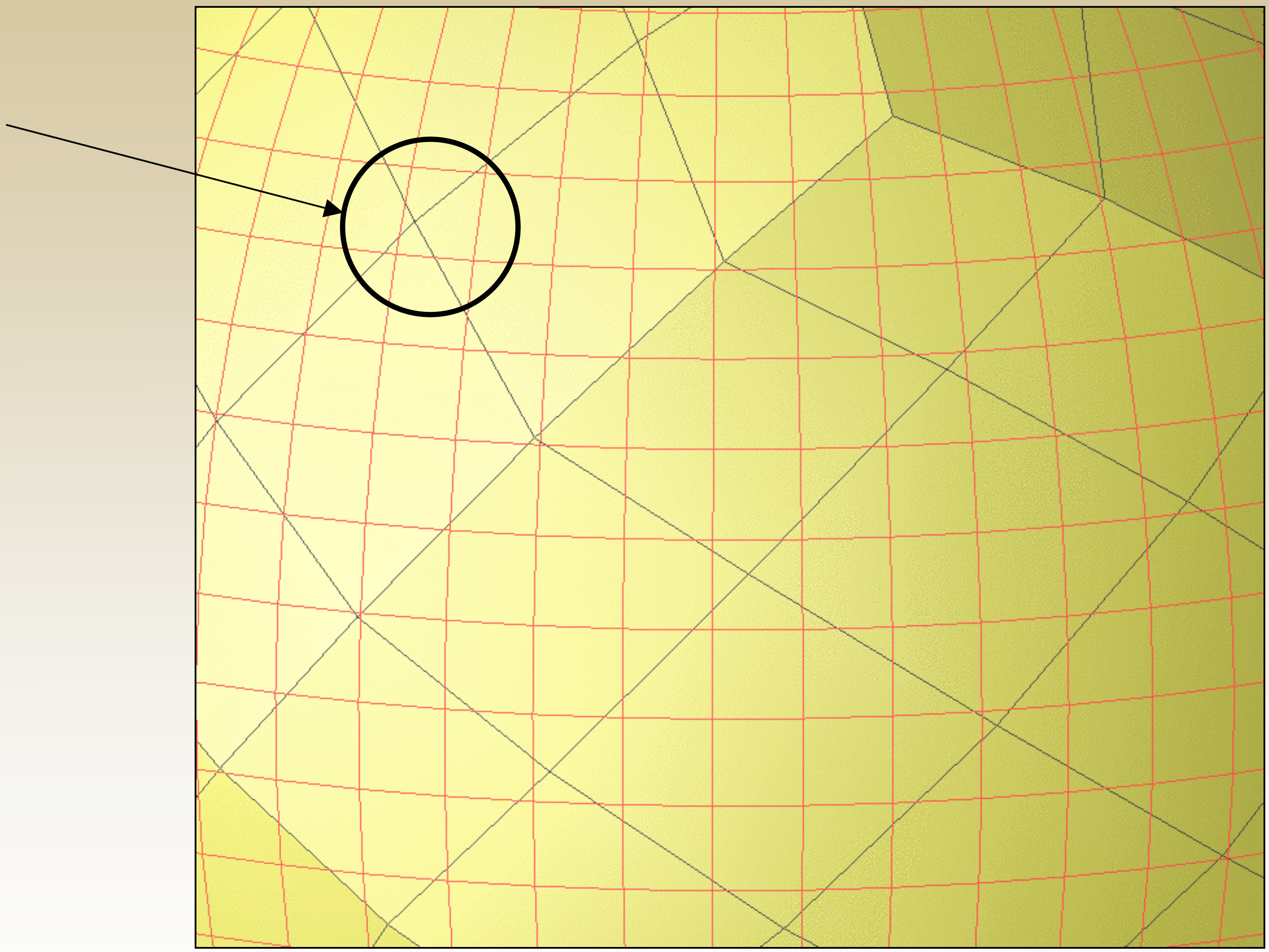

Interpolating velocity of a tracer

Code is flexible to encourage the user to easily install alternative methods.
Better methods may allow lower resolution for a particular problem.

Transform the great circle plane boundaries to rectangular boundaries using gnomonic transformation. This can be done and saved before the first timestep.

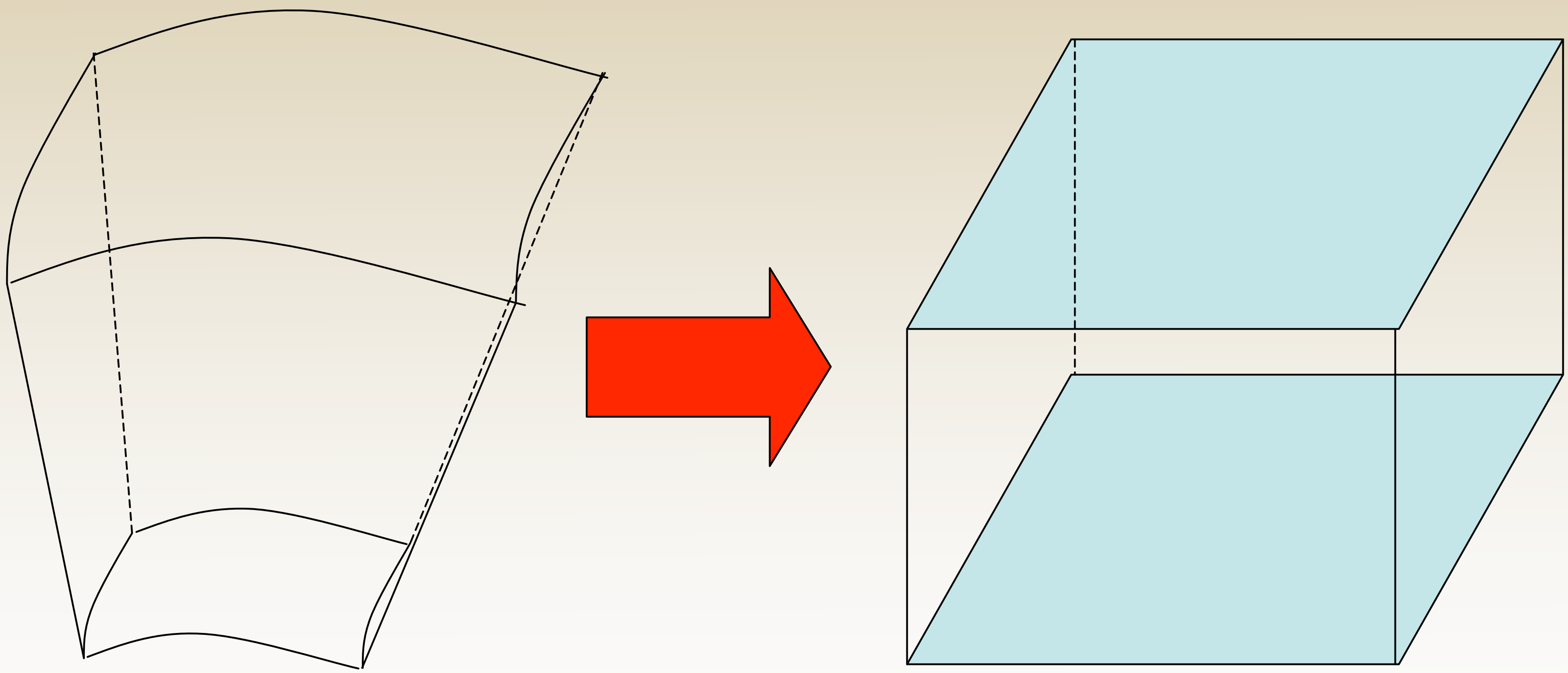

Transform theta, phi space to u,v space

Gnomonic Projection – great circles transform to straight lines

$$u = \frac{\cos\phi \sin(\lambda - \lambda_0)}{\cos c} \qquad v = \frac{\cos\phi_1 \sin\phi - \sin\phi_1 \cos\phi \cos(\lambda - \lambda_0)}{\cos c},$$

$$\boxed{\cos c = \sin\phi_1 \sin\phi + \cos\phi_1 \cos\phi \cos(\lambda - \lambda_0).}$$

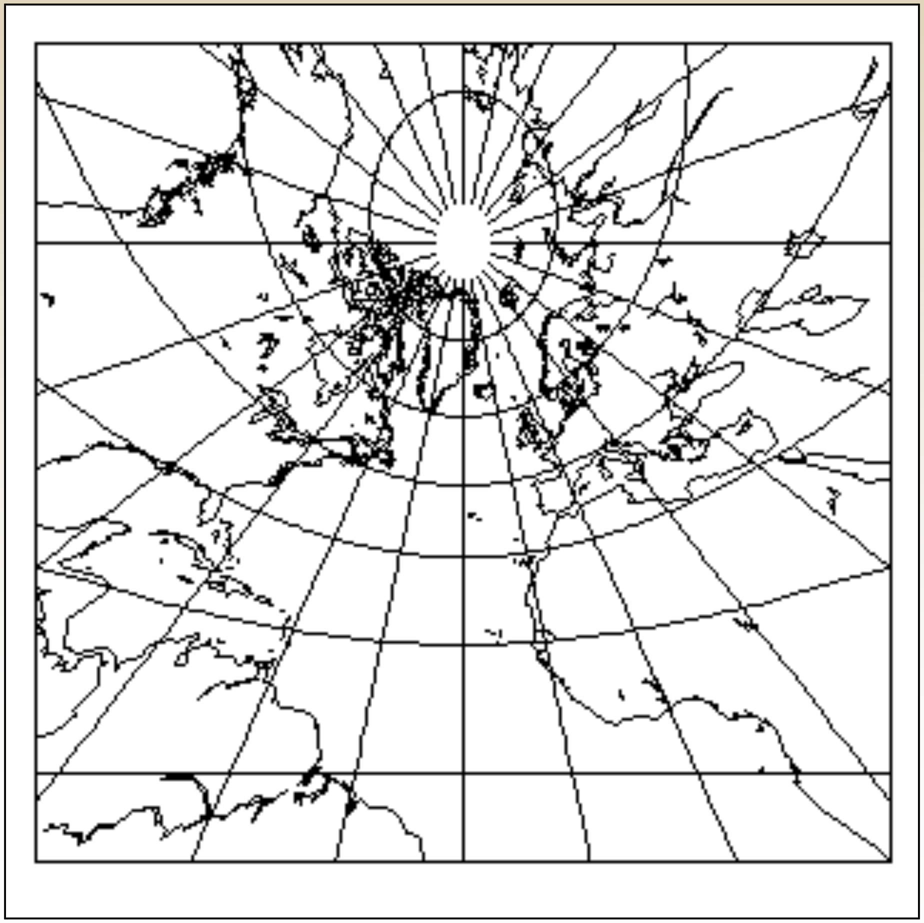

- Determine u and v for the tracer.

- Split upper and lower surfaces into 2 triangles each and determine which one the tracer is in.

- Using standard shape function methods for triangular elements, interpolate velocity for the tracer within each triangle.

- Weight by distance to upper and lower surfaces.

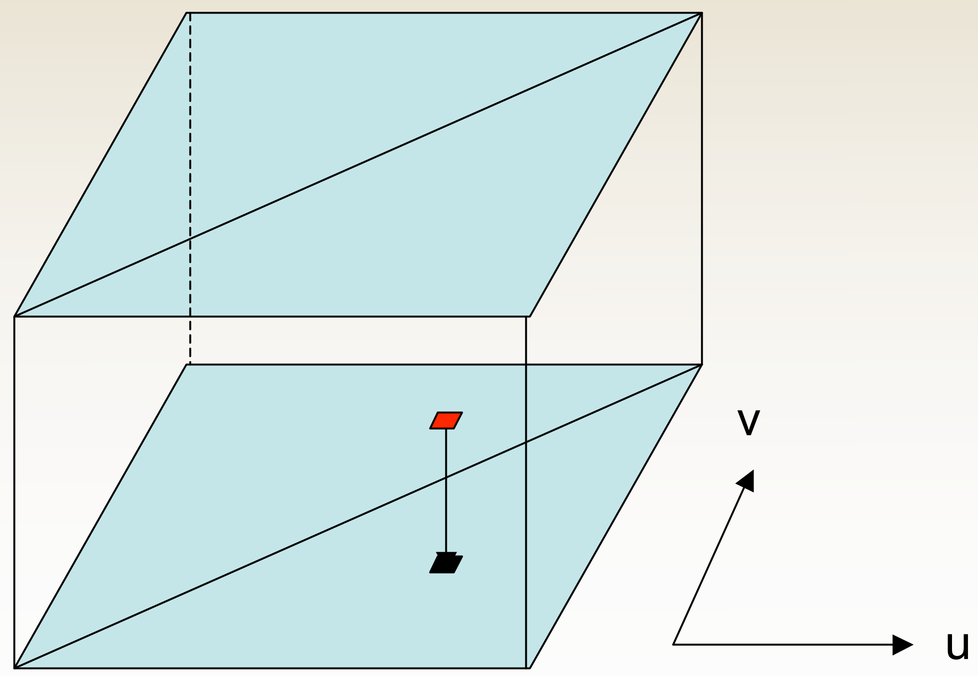

Advection Test (more rigorous than that in McNamara and Zhong (2004))

Vrad = 20.0 x radius * sin(phi)
Vtheta = 50.0 x radius * cos(phi)
Vphi = 120.0 radius *sin (theta)

Initial tracer position (theta=1.0; phi=0.0; radius=0.6)

Advect tracer from time=0.0 to time=0.8
pathlength ~ 132 mantle thicknesses (381,480 km)

Timestep determined by Courant Criterion

Mesh	steps	difference	Diff/length
Analytical 4RK	80 million		
12x33x33x33	9,166	51 km	0.013%
12x48x48x48	13,861	23 km	0.006%
12x64x64x64	18,554	13 km	0.003%

1. Common components of tracing in geodynamical codes
    - Comments about tracing in CitcomS
      (thermochemical extension released in 2007)
2. Common uses for tracers, along with research examples
    - Deformation tracking
        - Example (providing a framework for seismic anisotropy prediction)
    - Thermochemical convection
        - Example (small-scale ULVZ modeling)
    - Multiple rheologies
        - Example (lithospheric strength and crustal weakness)

3. Investigating large scale mantle convection using thermochemical convection
    - Modeling thermochemical piles and plume clusters
    - Investigating tomography as a constraint (Abigail Bull)
    - Investigating CMB topography as a constraint (Teresa Lassak)

Tracking deformation to predict seismic anisotropy

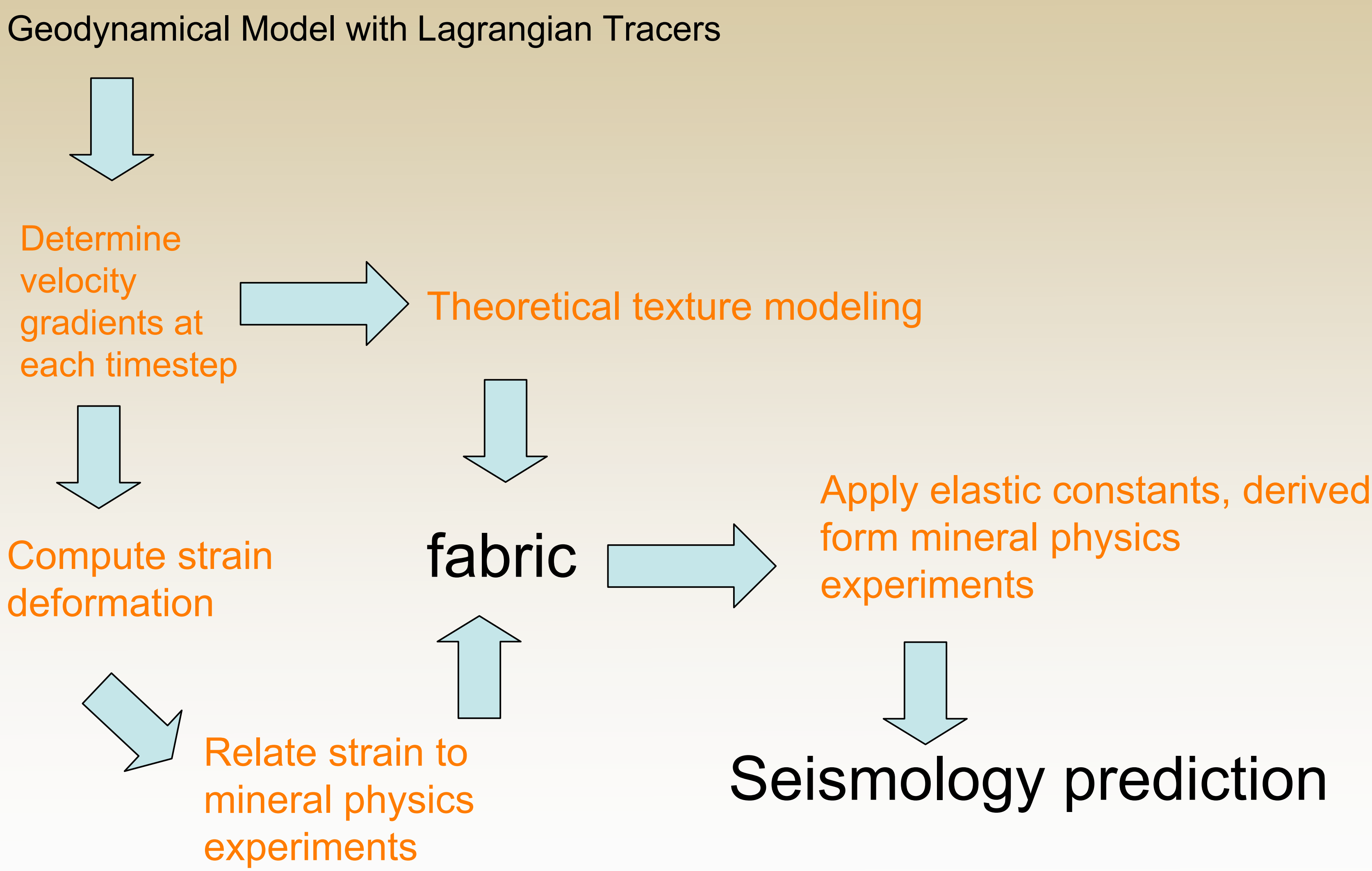

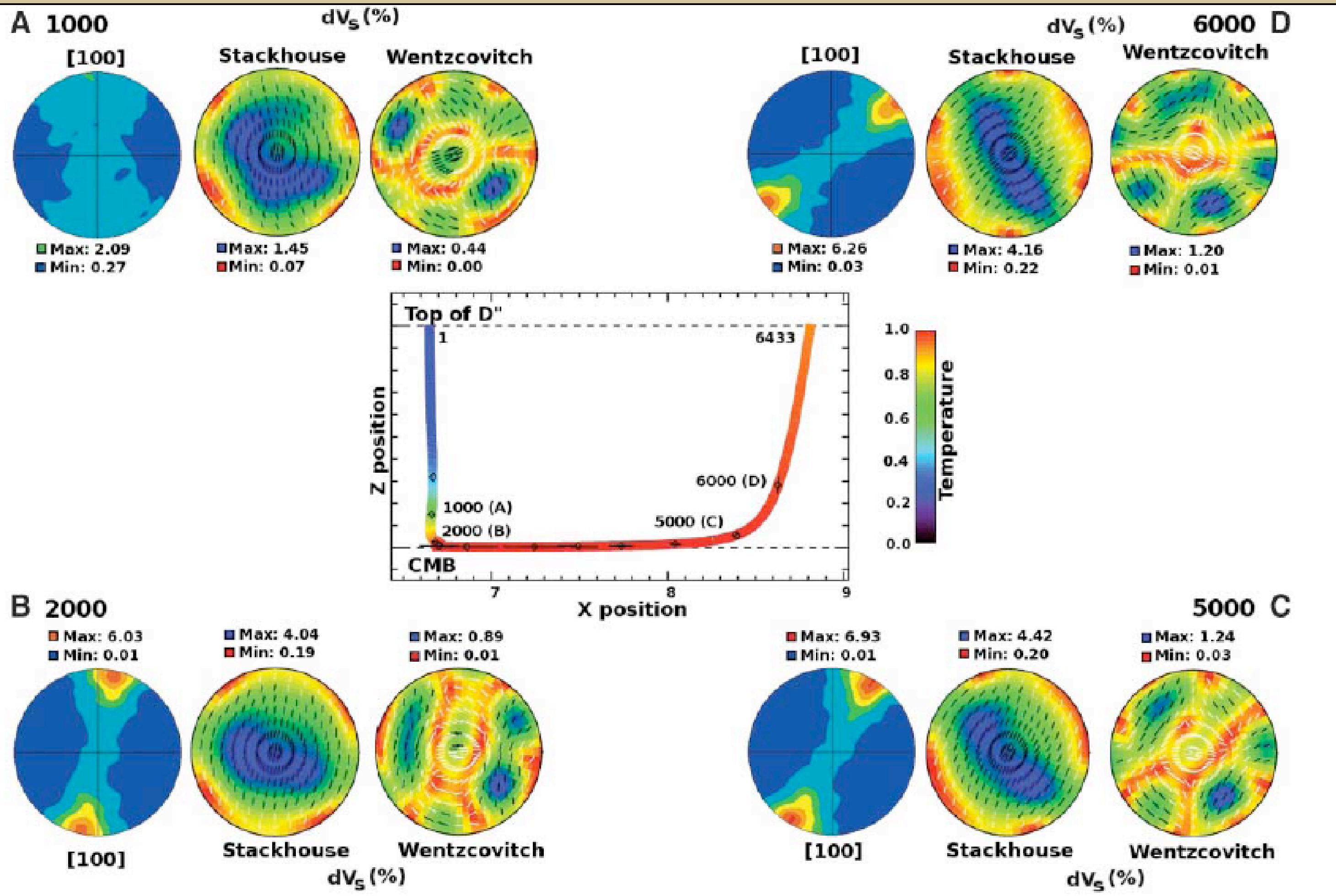

Fig. 3. Modeled temperature, strain, texture, and shear wave splitting from silicate post-perovskite in D″. The central figure illustrates the evolution of temperature and strain along a streamline. Temperatures are normalized so that $T = 0$ at Earth's surface and $T = 1$ at the CMB, strains are indicated by the black lines representing the evolution of maximum and minimum stretch of the Lagrangian particle for every 500 time steps, and numbers are time-step numbers. Panels (**A**) to (**D**) present the modeled 3D [100] orientations, shear wave splitting dV_S, and fastest shear wave polarizations at time steps 1000, 2000, 5000, and 6000, respectively. Shear wave splitting was calculated using the elastic moduli of Stackhouse *et al.* (*24*) and Wentzcovitch *et al.* (*25*). Linear scale, equal area projection. Contours for the [100] and dV_S pole figures are expressed in multiples of a random distribution and percentage, respectively. Black and white lines (for low and high anisotropies, respectively) indicate the direction of polarization of the fast shear wave.

(Merkel et al, 2007)

It takes time (i.e. a certain amount of deformation) to generate fabric

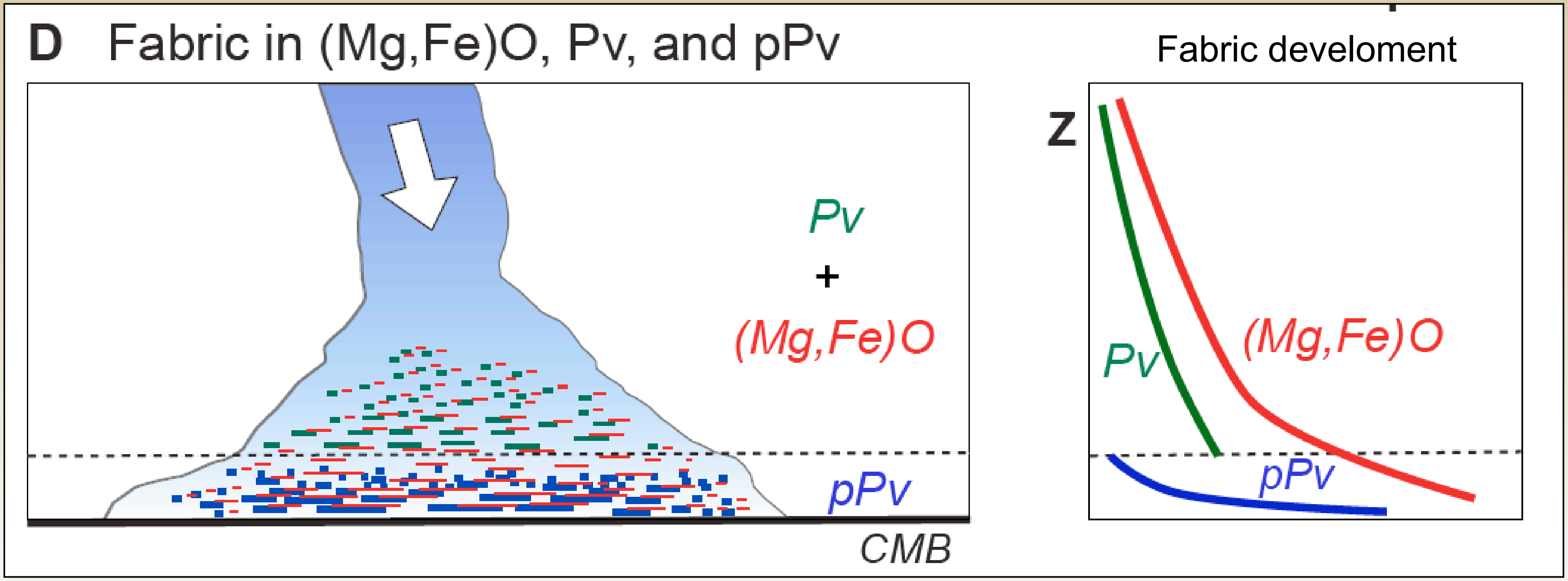

Garnero and McNamara (2008)

Collaborative work with Rudy Wenk and Barbara Romanowicz to predict lowermost mantle seismic anisotropy from geodynamical deformation.

Geodynamical calculations, theoretical texture modeling, synthetic waveform modeling

Goals:

- Explore how different deformation mechanisms, mineral assemblages, and elastic constants associated with magnesiowustite, perovskite, and pPv are expected to affect seismic anisotropy for different tectonic regions.
- In regions of abundant seismic anisotropy observations, can we use this method to differentiate between mineral physics assumptions?
- By exploring different tectonic regions geodynamically, can we use this method to propose future seismology experiments that help constrain lower mantle dynamics?
- Develop an efficient means to provide geodynamic data for mineral physics calculations
    - Online storage of data
    - Full description of data, particularly dimensional scaling
    - Provide visualization to aid in tracer choosing

We start with a case in which we examine the deformation of lowermost mantle material that is swept into mantle plumes.

CitcomCU, 32 processors, 8.4 M elements, Ra = 5×10^8

rheology: 50x jump across TZ, 100,000x contrast due to temperature-dependence.

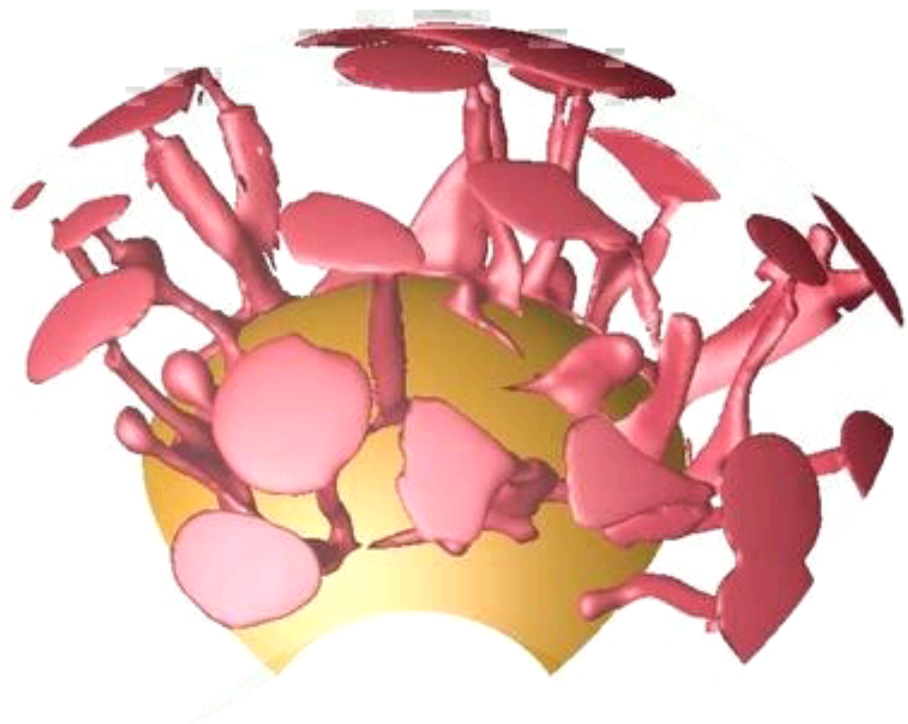

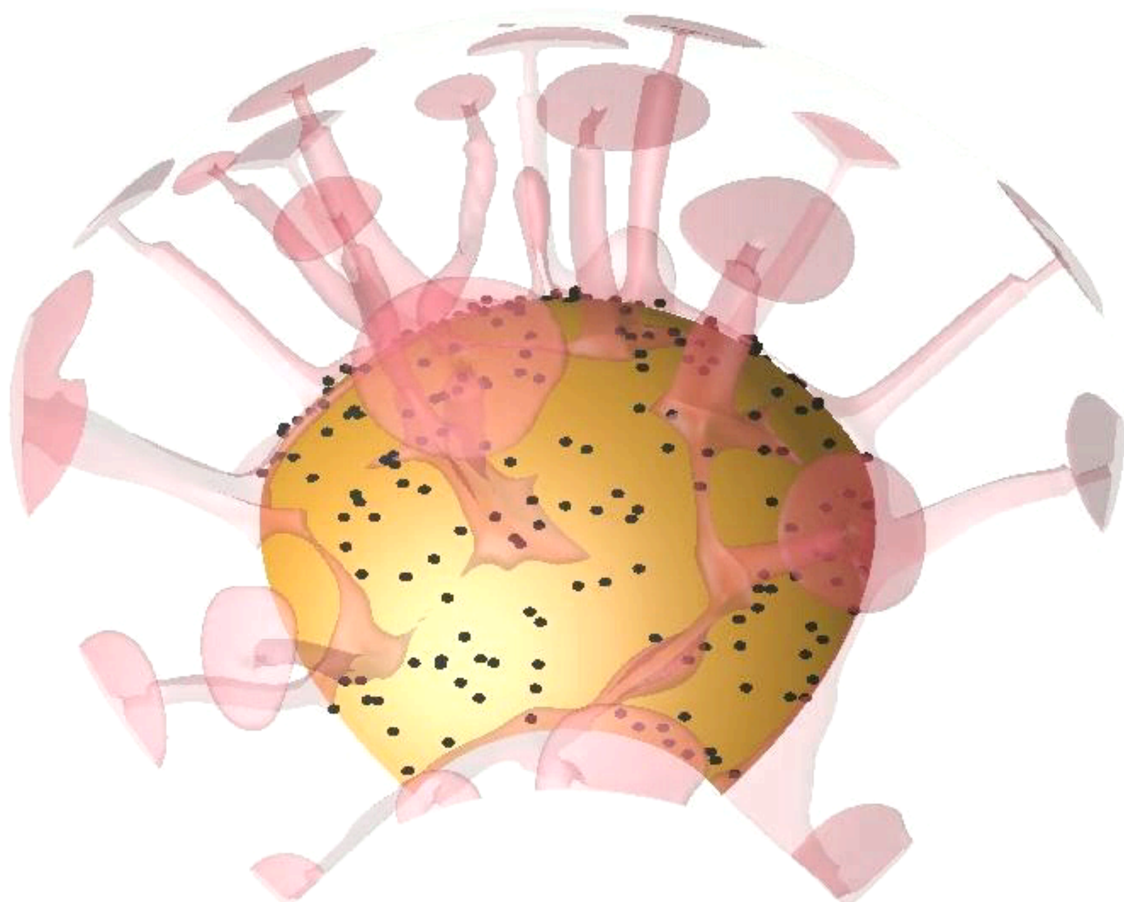

www.mcnamara.asu.edu/geodynamical_deformation/mantle_plumes/

Small scale ultra-low velocity zones at the CMB

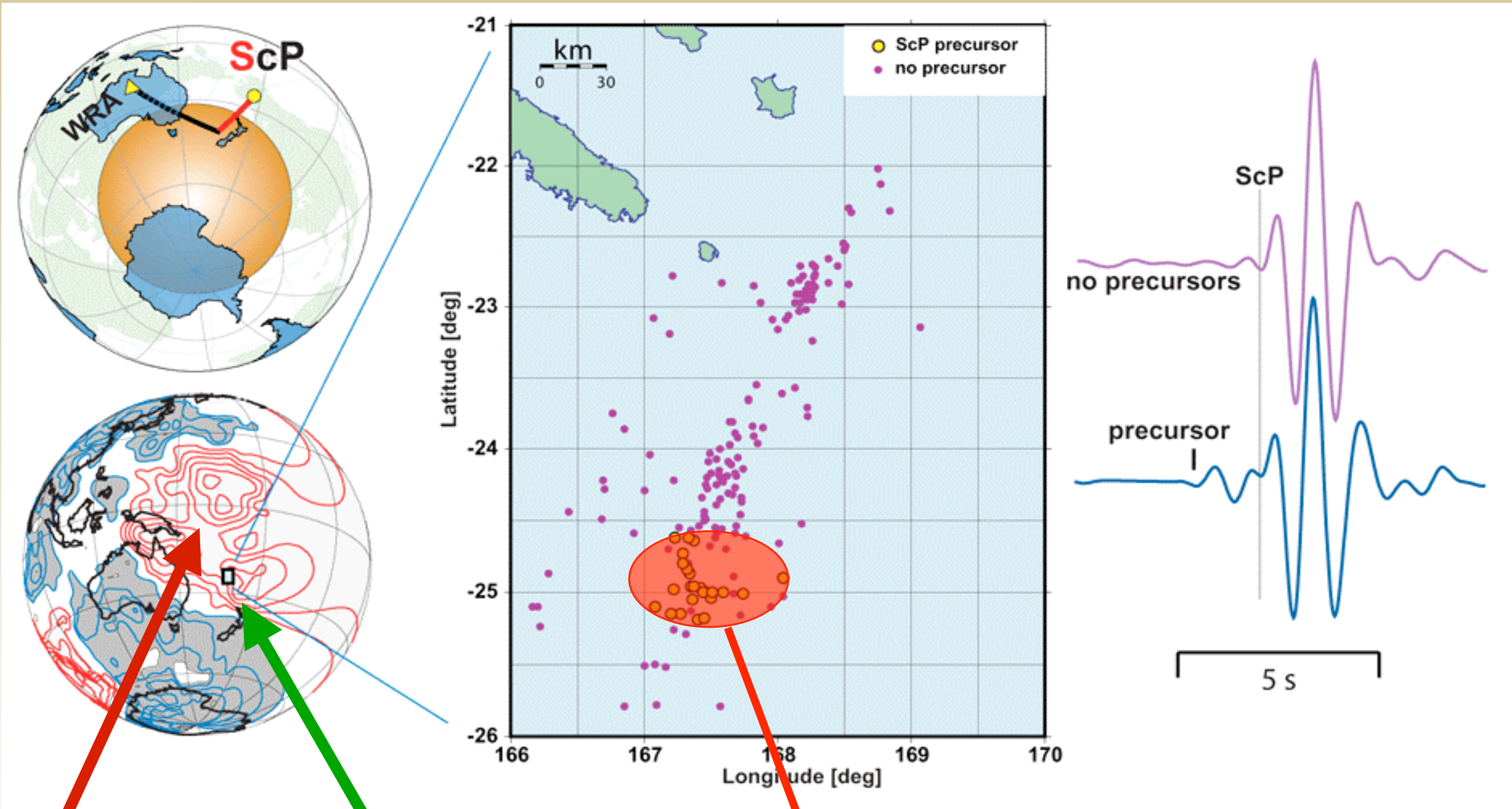

tomography low shear velocity

study near edge of anomaly

- **Best-fit ULVZ model properties:**
  - **Thickness : 8.5 (±1) km**
  - **dV_P : -8 (±2.5) %**
  - **dV_S : -25 (±4) %**
  - **dρ : +10 (±5) %**

Rost, Garnero, Williams, Manga [*Nature,* 2005]

Hypothesis of lowermost mantle dynamics, based on seismological observations.
The main concerns were: can such high densities be supported? Where should ULVZ reside within piles?

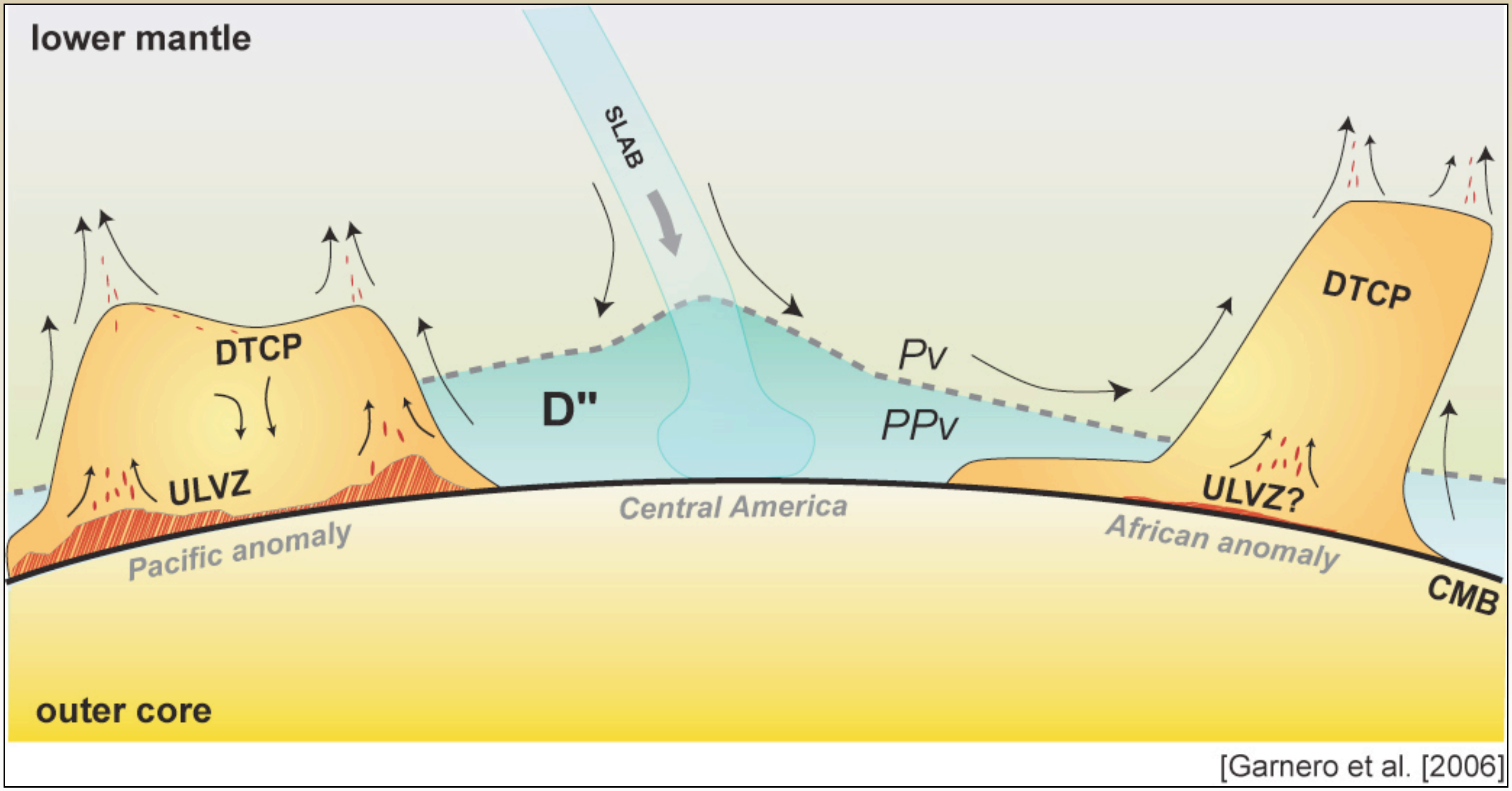

Geodynamic study, in collaboration with Ed Garnero and Sebastian Rost, to investigate the following:

[Assuming that ULVZ is due to chemical heterogeneity with/or without melt]

(See Hernlund and Tackley 2007 for cases in which melt is the cause of ULVZ)

1) Can viscous stresses support topography on a small volume of very dense material at the CMB, consistent with observational modeling?
2) If thermochemical piles exist, where would ULVZ reside with respect to the piles?
3) If thermochemical piles do not exist, can plumes support ULVZ topography? Can plumes act to sweep ULVZ material into larger reservoirs?

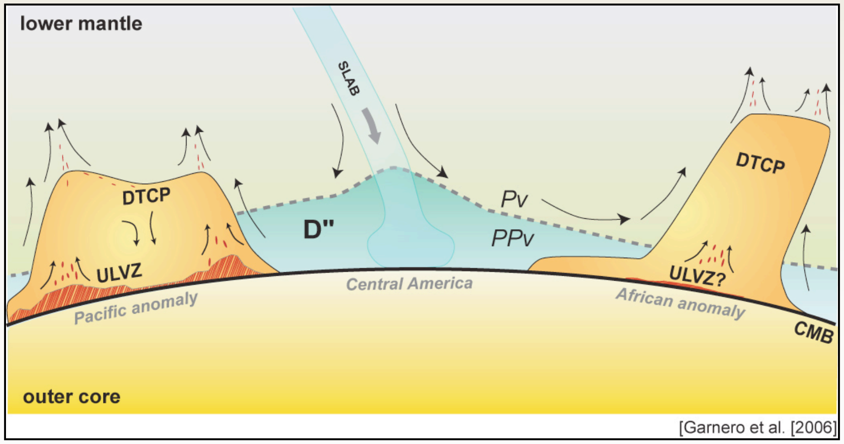

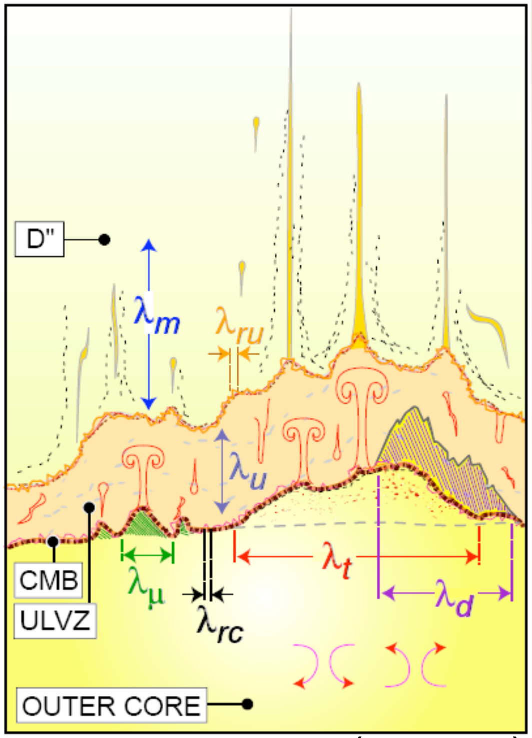

(garnero)

METHOD

High resolution 2D thermochemical convection modeling of whole mantle convection in a Cartesian geometry (2 km resolution in the lowermost portion) using thermochemical version of finite-element code Citcom.

Rayleigh number, Ra = 5x107

Temperature- and Depth-dependent viscosity

- 50x viscosity jump at the 660
- viscosity contrast due to temperature = 10,000x

Composition - 3 component system

- Thermochemical piles
  - Intrinsic density increase 2.0-7.2% (B=0.8)
  - Volume: equivalent to a 290 km layer
- ULVZ material
  - Intrinsic density increase 2.5-45.0% (B=1.0-5.0)
  - Volume: equivalent to a 5 km layer

CASE 1 ULVZ Material B=1.0 (~2.5-9% density increase)

Significant entrainment of the ULVZ material occurs

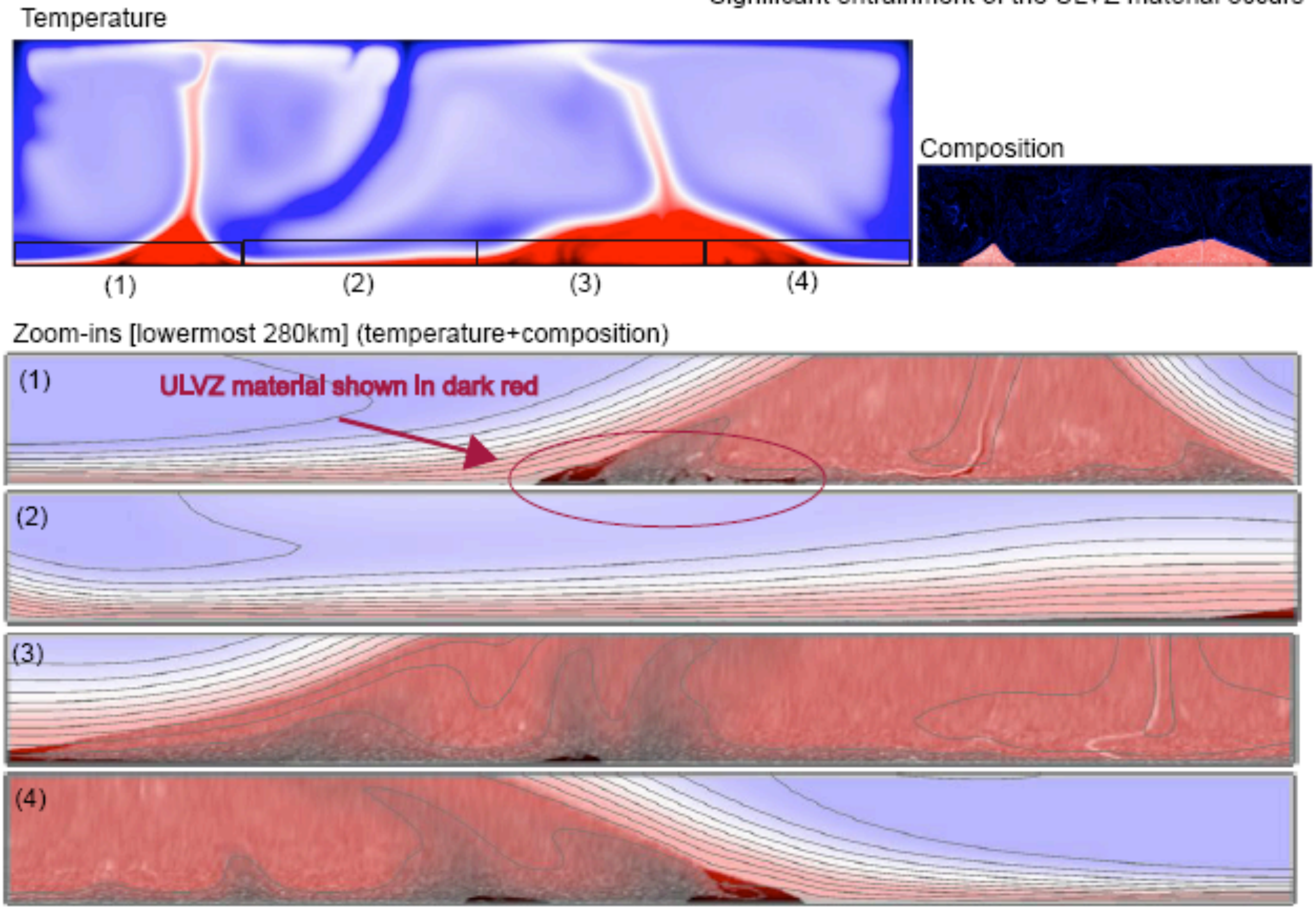

CASE 2 ULVZ Material B=2.0 (~5-18% density increase)

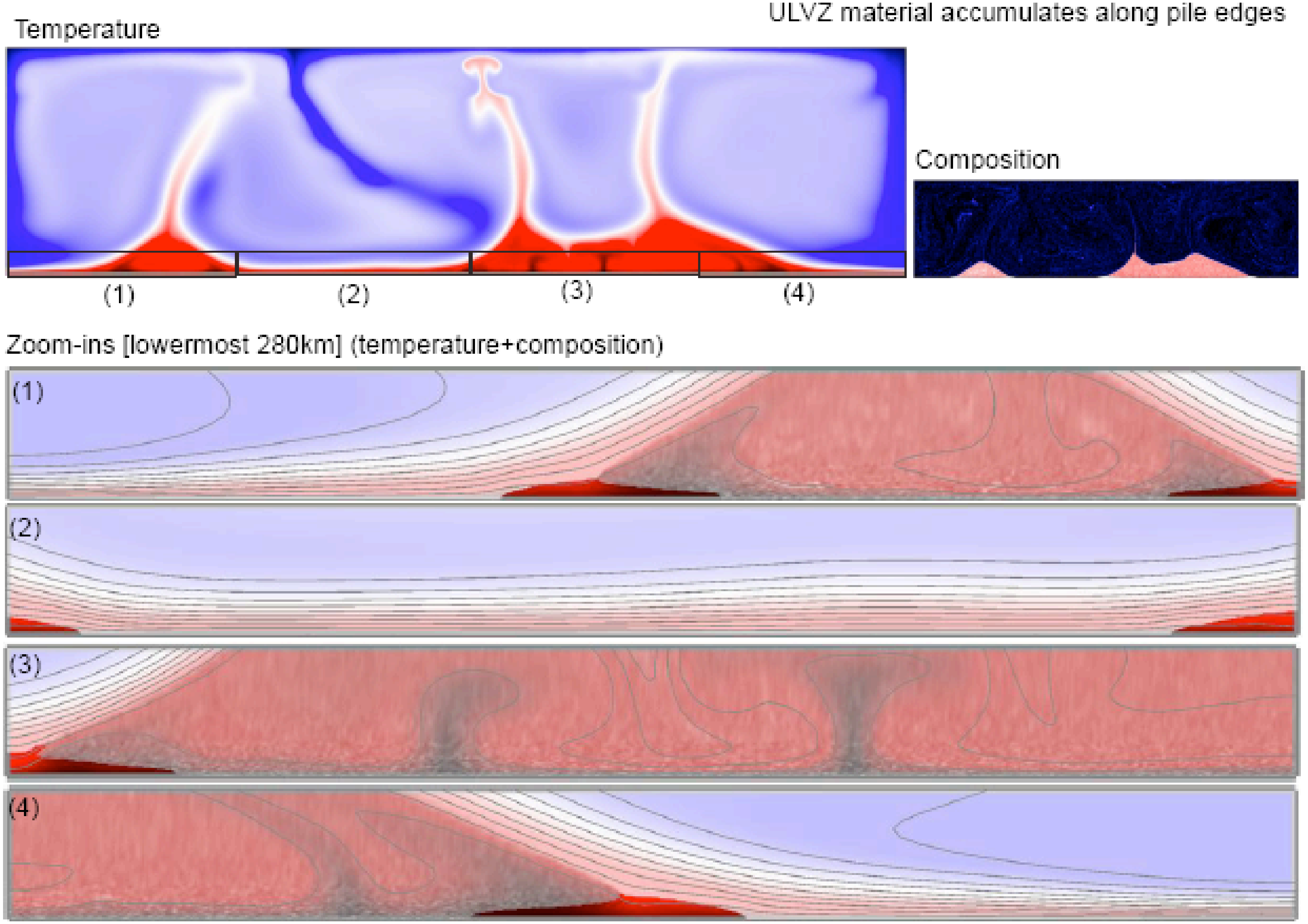

CASE 3 ULVZ Material B=4.0 (~10-36% density increase)

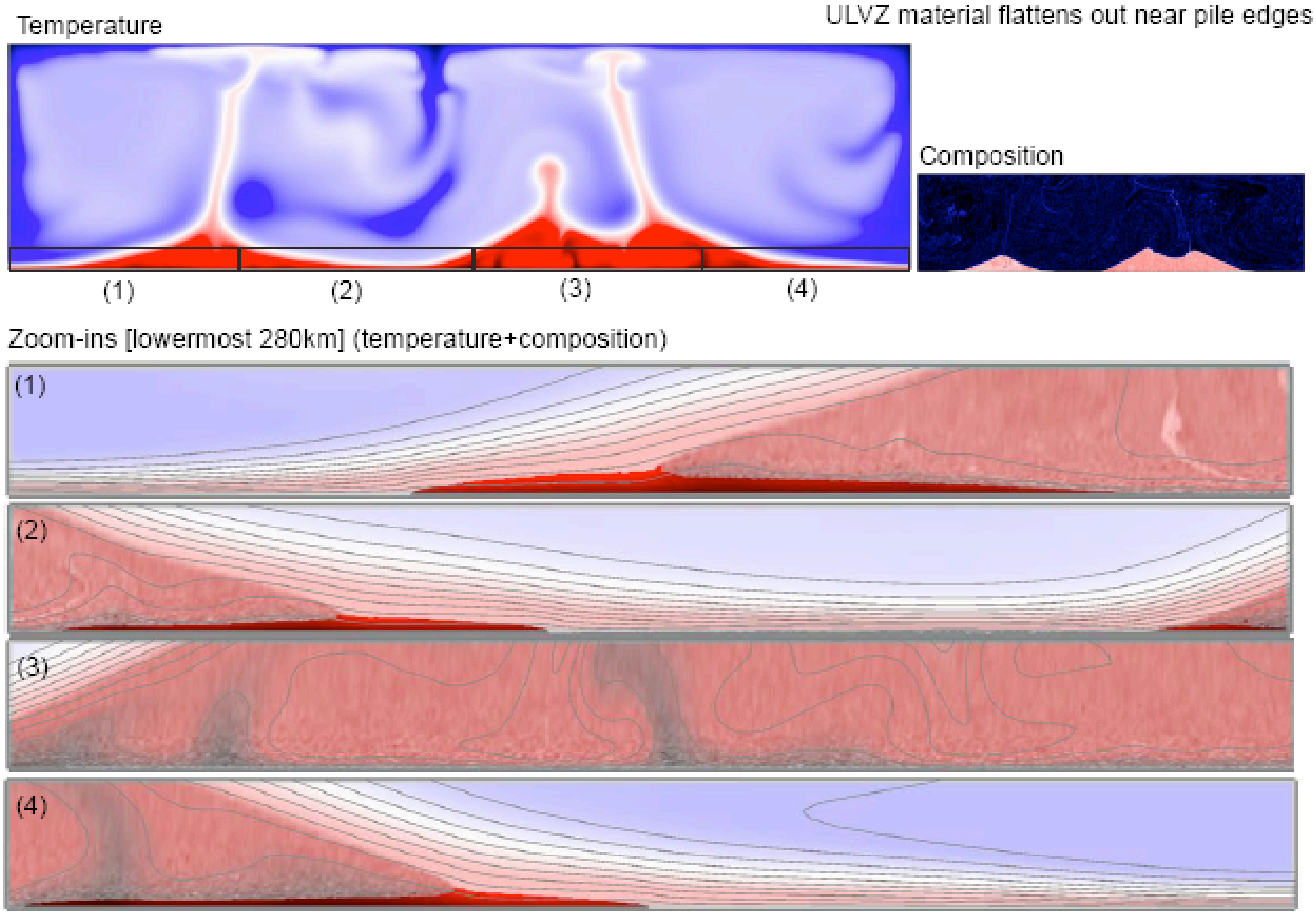

CONCLUSIONS

1. Mantle convection can dynamically support (create topography) on a small volume of high density mantle material. The “small volume” is key; for the densities investigated here, much larger volumes would flatten out into a layer over the CMB.

2. The density must be greater than B=1.0 to avoid getting entrained into the surrounding mantle.

3. If ULVZ is caused by chemical heterogeneity (as modeled here), and if thermochemical piles exist, it is expected that the ULVZ will accumulate at the edges of the piles.

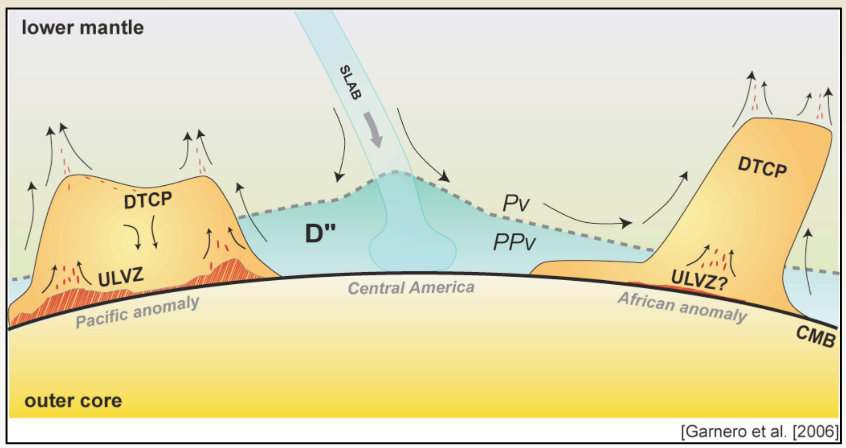

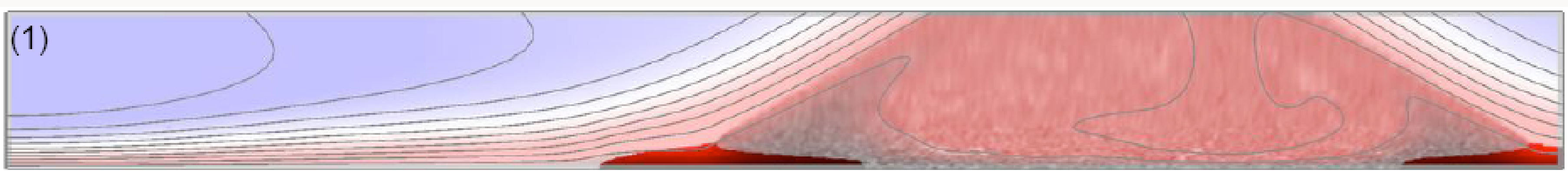

ULVZ resides in upwelling regions, so its distribution may be an indicator to the type of convection

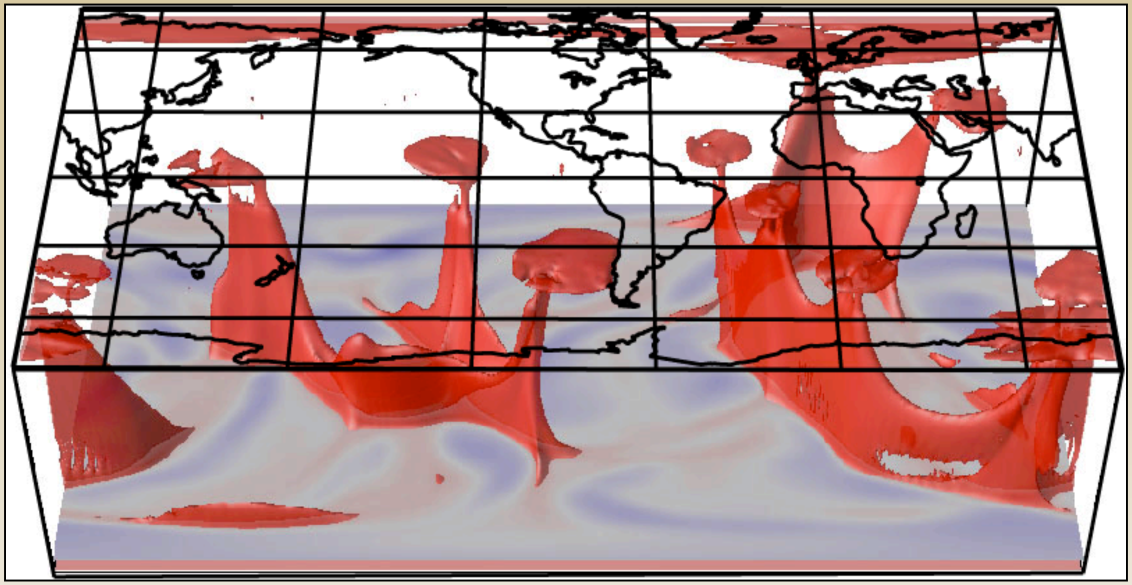

Plume Clusters

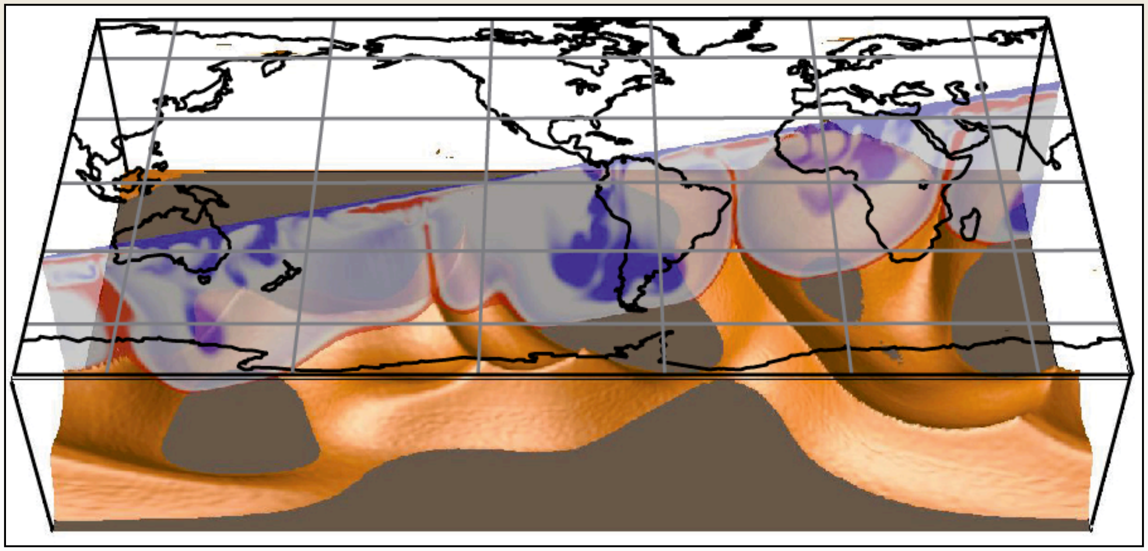

Thermochemical Piles

ULVZ resides in upwelling regions, so it's distribution may be an indicator to the type of convection

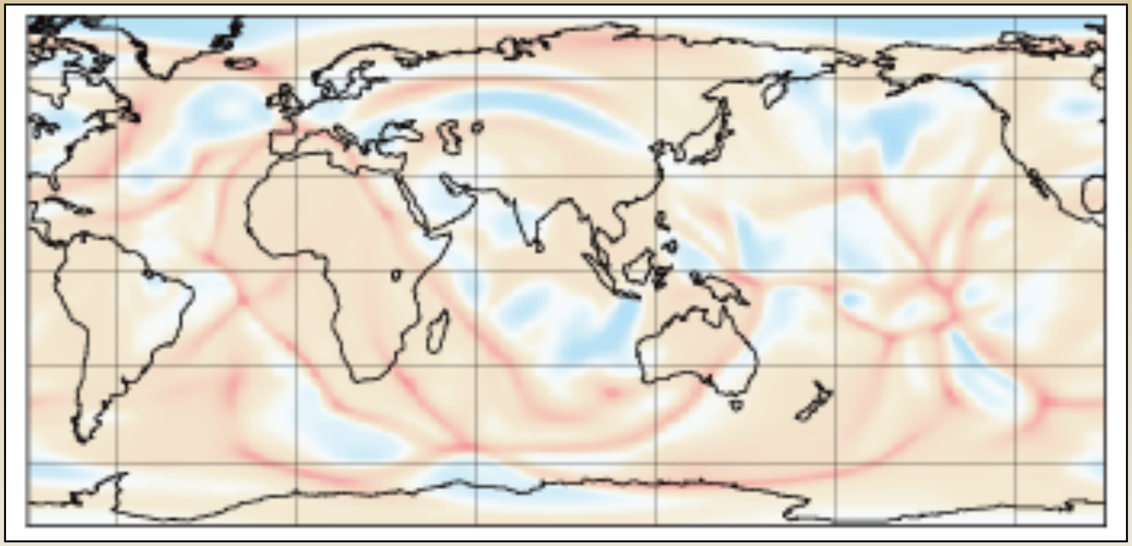

Plume Clusters

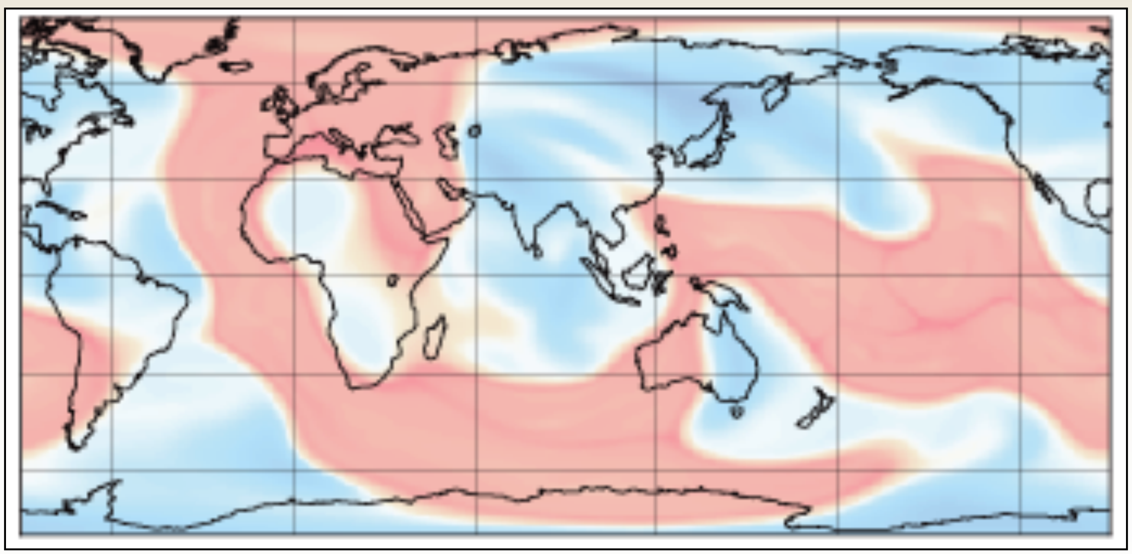

Thermochemical Piles

1. Common components of tracing in geodynamical codes
    - Comments about tracing in CitcomS
      (thermochemical extension released in 2007)
2. Common uses for tracers, along with research examples
    - Deformation tracking
        - Example (providing a framework for seismic anisotropy prediction)
    - Thermochemical convection
        - Example (small-scale ULVZ modeling)
    - Multiple rheologies
        - Example (lithospheric strength and crustal weakness)

3. Investigating large scale mantle convection using thermochemical convection
    - Modeling thermochemical piles and plume clusters
    - Investigating tomography as a constraint (Abigail Bull)
    - Investigating CMB topography as a constraint (Teresa Lassak)

?

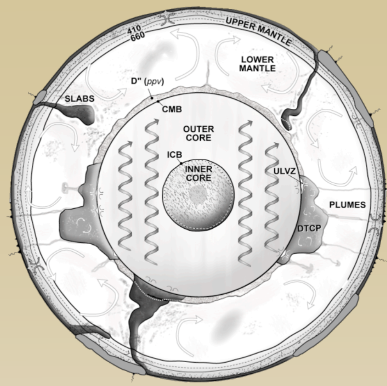

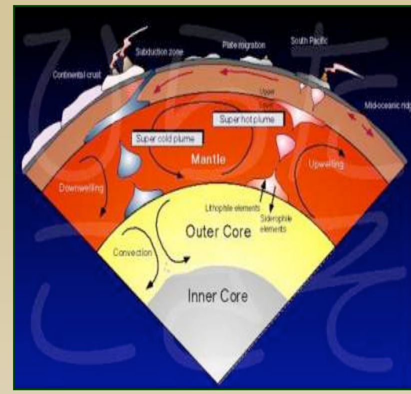

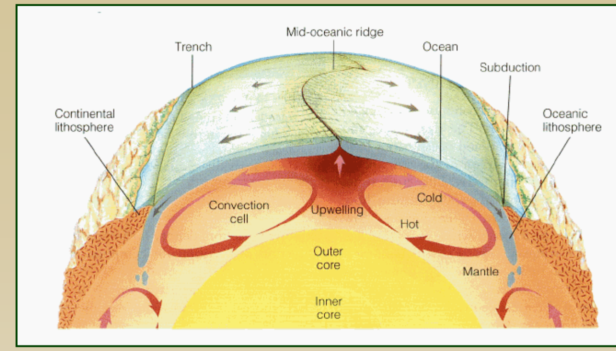

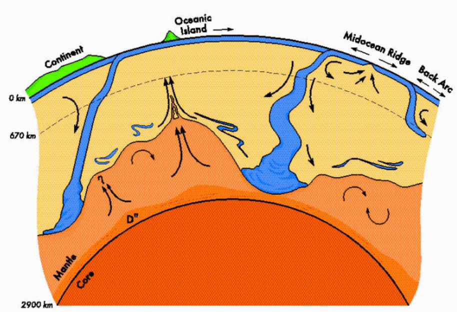

(Kellogg et al., 1999)

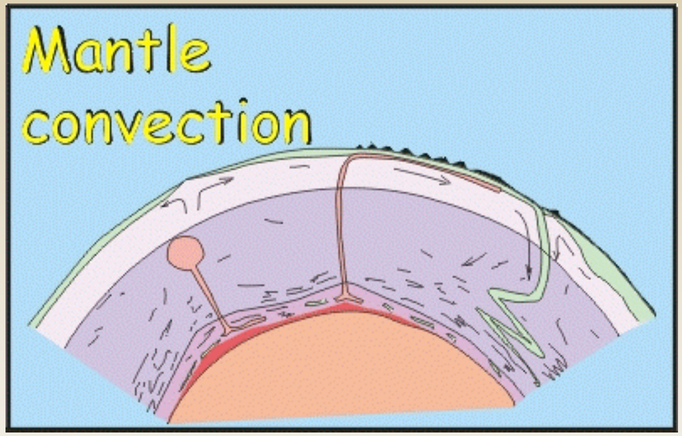

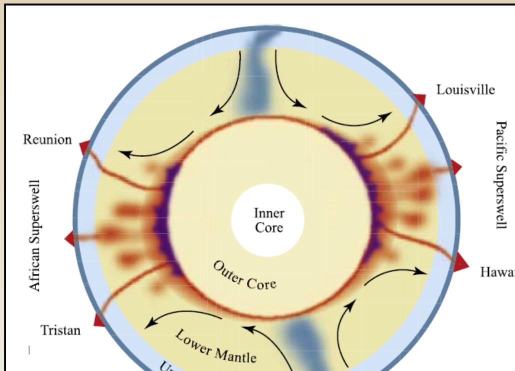

(Jellinek and Manga, 2004)

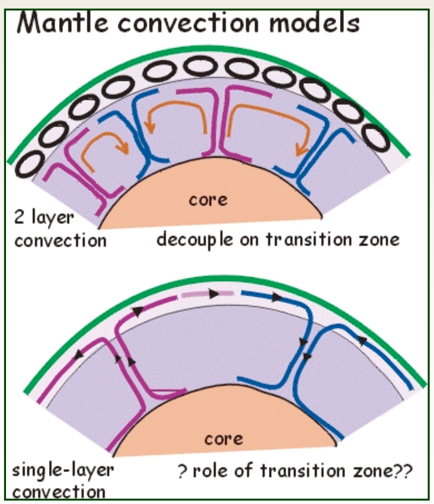

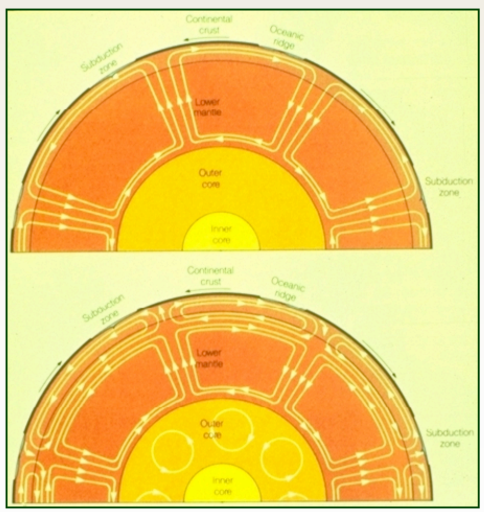

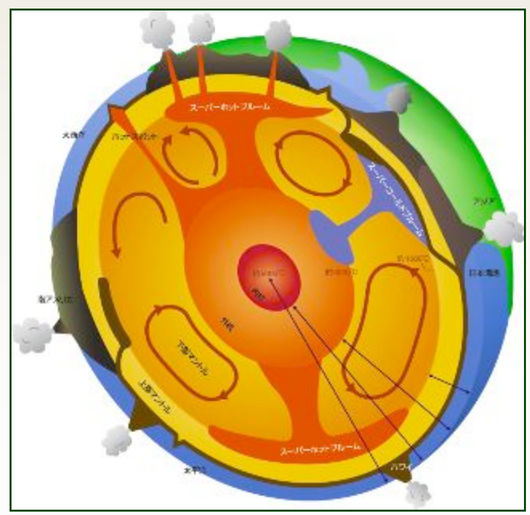

Seismic Tomography

Model S20RTS (Ritsema et al., 1999, 2004)

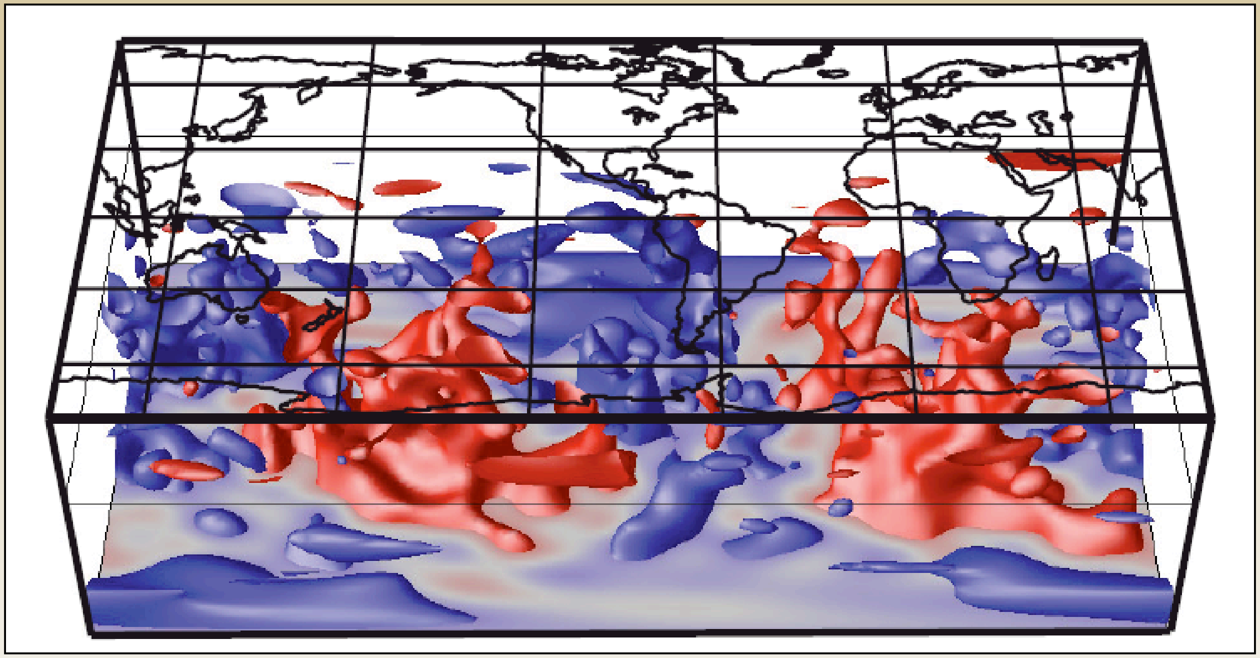

Isosurfaces

Red 0.6% slower than average

Blue 0.6% faster than average

Map near CMB

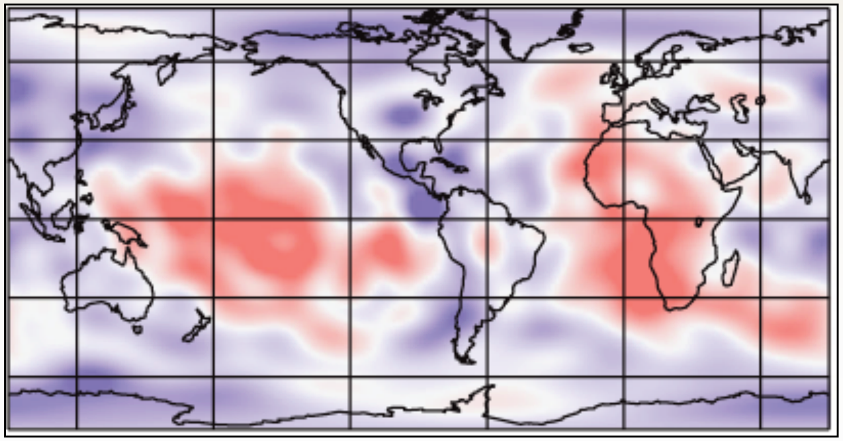

Additional Seismic Studies infer Chemical Heterogeneity in the lower mantle:

[eg., Ishii and Tromp, 1999; 2004; Masters et al., 2000; Forte and Mitrovica, 2001; Ni et al., 2002; Ni and Helmberger, 2003; Trampert et al., 2004; Wang and Wen, 2004; To et al., 2005; Ford et al., 2006]

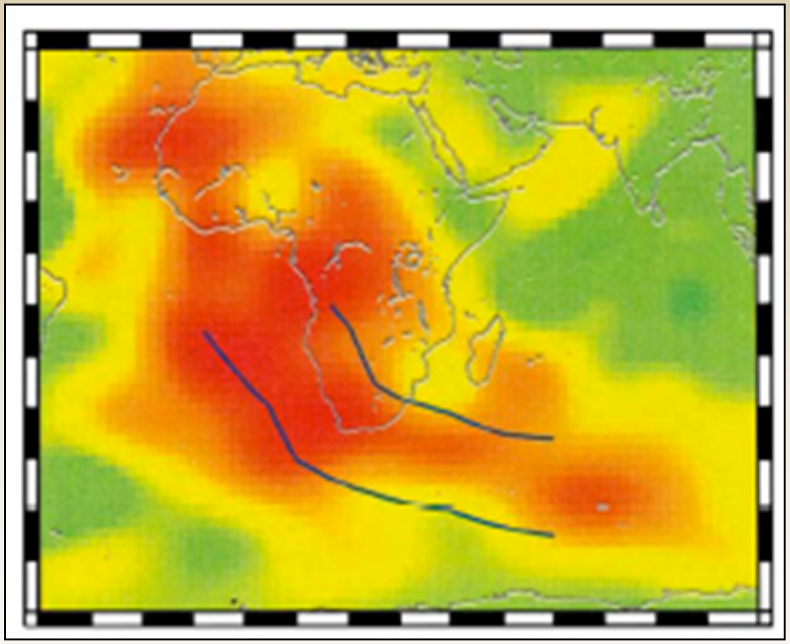

(Ni and Helmberger, 2003)

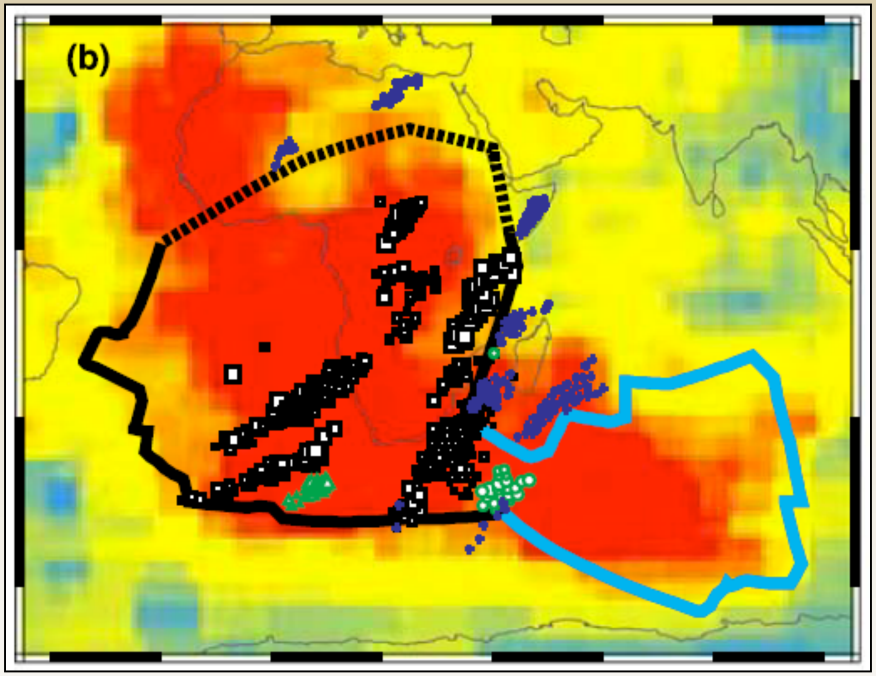

(Wang and Wen, 2004)

Many geodynamical have been performed to understand the effect of chemical heterogeneity on mantle convection

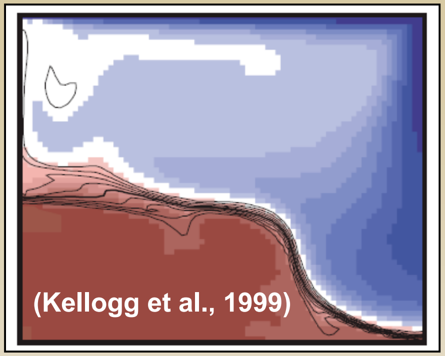
(Kellogg et al., 1999)

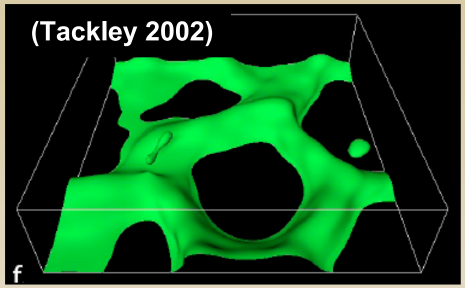
(Tackley 2002)

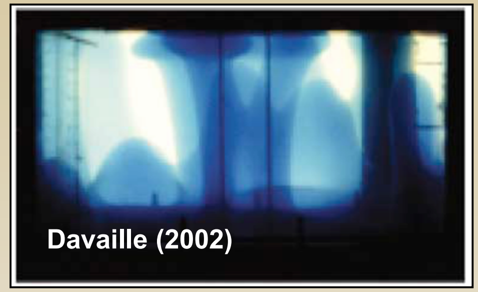
Davaille (2002)

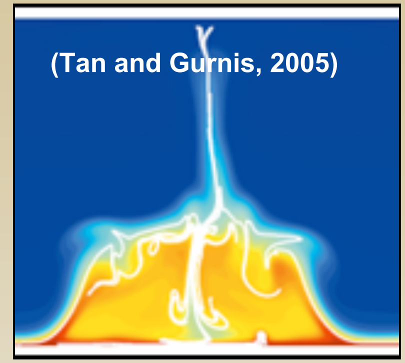
(Tan and Gurnis, 2005)

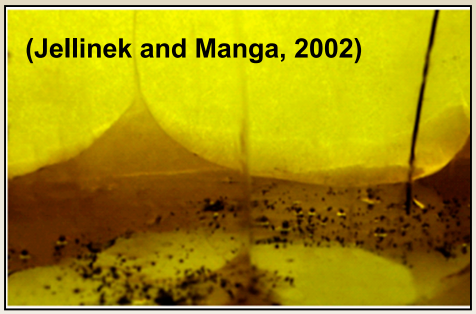
(Jellinek and Manga, 2002)

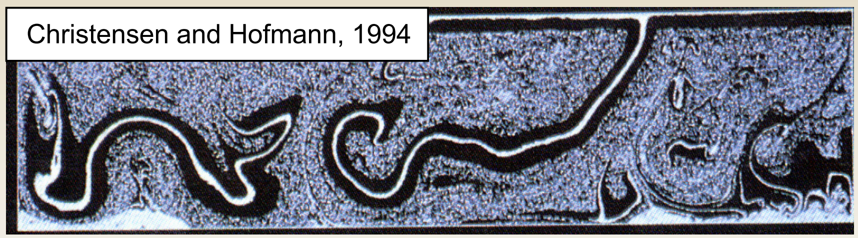
Christensen and Hofmann, 1994

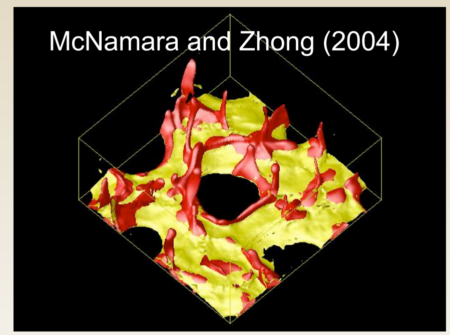
McNamara and Zhong (2004)

Some Important Questions:

How does chemical heterogeneity affect the driving forces?

How does chemical heterogeneity affect heat transport through the mantle?

What is the source of chemical heterogeneity?

Dynamical Hypotheses

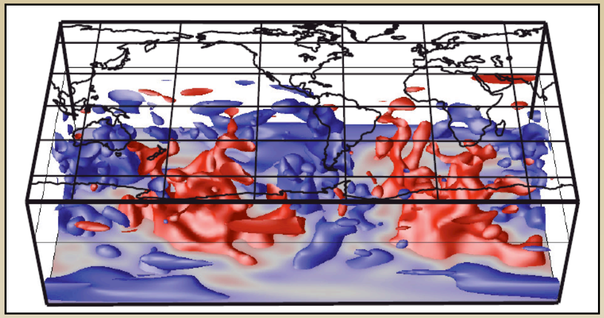

S20RTS (Ritsema et al., 1999; 2004)

Plume Clusters

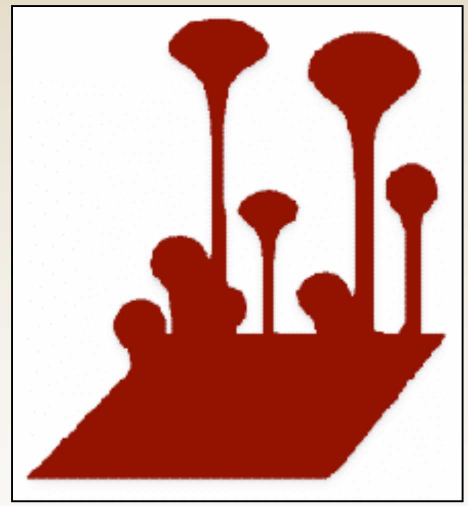

Schubert et al. (2004)

Thermochemical Piles

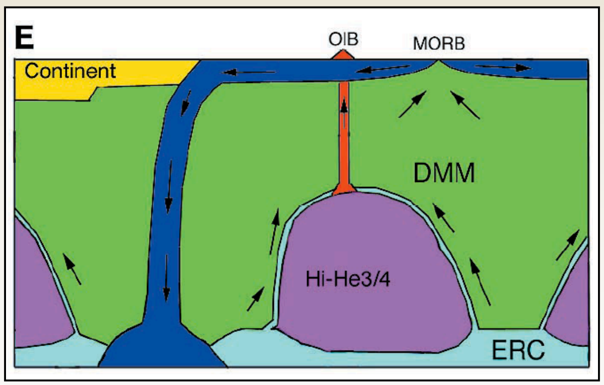

Tackley (2000)

Thermochemical Superplumes

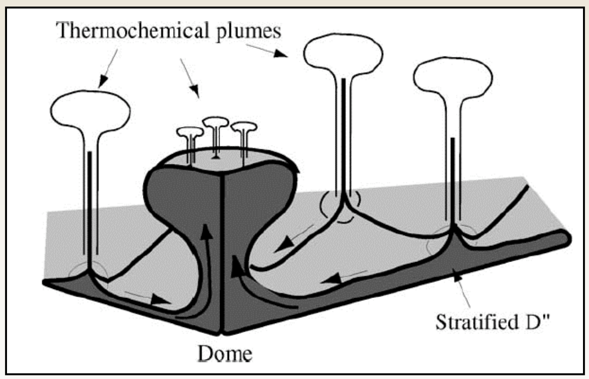

Davaille (2002)

Understanding the cause of the African and Pacific anomalies is central to this debate

Thermochemical geodynamical models:

❑ Involves the presence of a more-dense (~3-6%) mantle reservoir.

❑ 2 competing buoyancy forces:

- ➢ intrinsic density
- ➢ density decrease due to thermal expansion.

Thermochemical Superplumes:

net upward buoyancy

unstable, short-lived

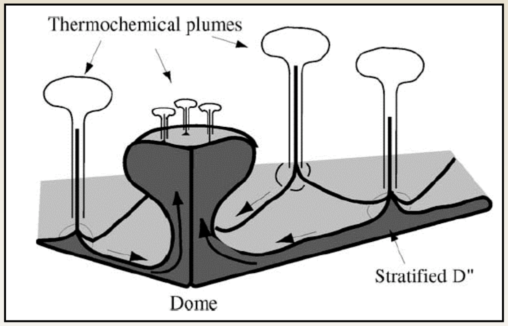

Thermochemical Piles:

near neutral buoyancy

stable, long-lived

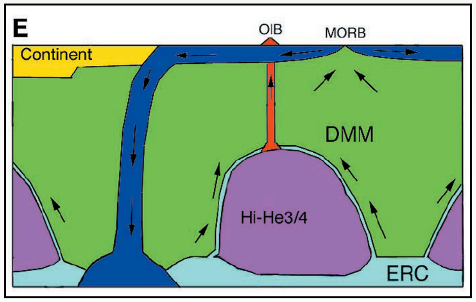

The source of the heterogeneity can have a strong effect on entrainment, morphology, and heat transport

temperature

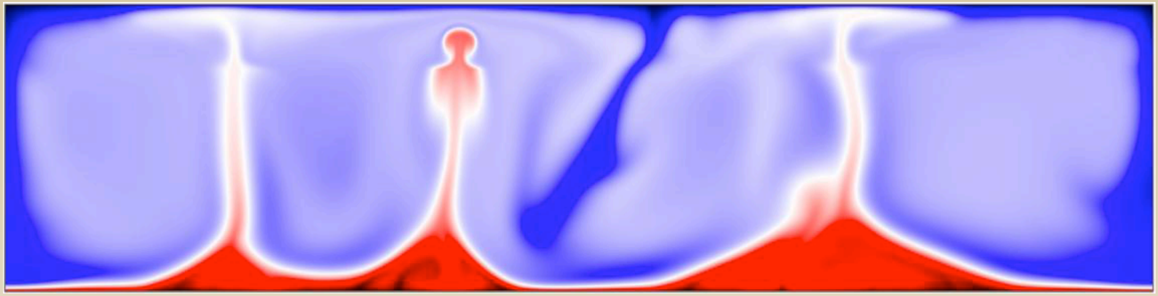

composition

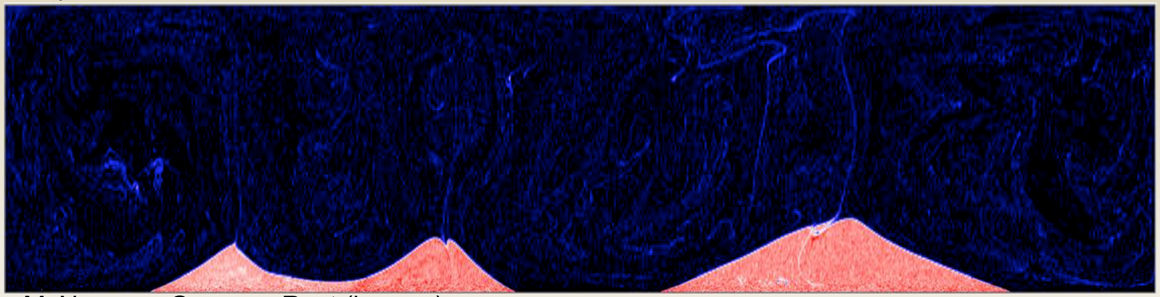

McNamara, Garnero, Rost (in prep)

Primordial Piles
➢Relatively homogeneous entrainment
➢Sharp sides and tops
➢Large temperature gradients across sharp boundary

Piles made by segregated oceanic crust
➢Heterogeneous entrainment
➢Sharp lower sides, diffuse tops
➢Lower temperature gradients across diffuse boundary

Temperature (color) and composition (darkness)

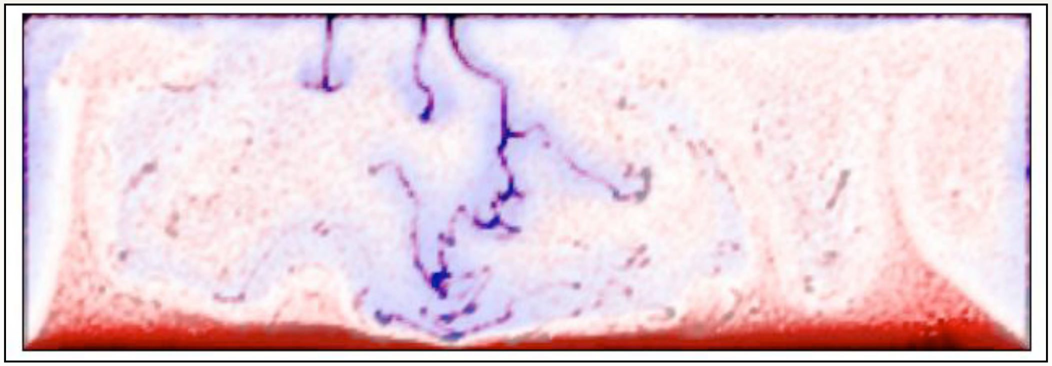

(McNamara and Garnero, 2008)

Plume Clusters may be imaged poorly by tomography, appearing as large anomalies

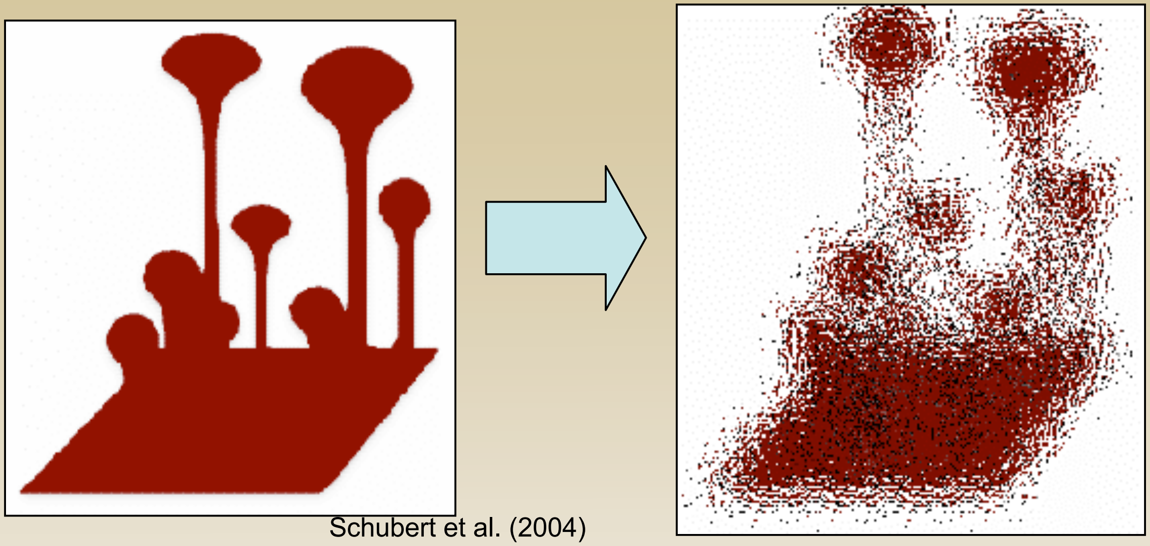

Schubert et al. (2004)

Plume Clusters don’t necessarily imply lack of chemical heterogeneity; instead, heterogeneity is such that it doesn’t inhibit the formation of small-scale plumes.

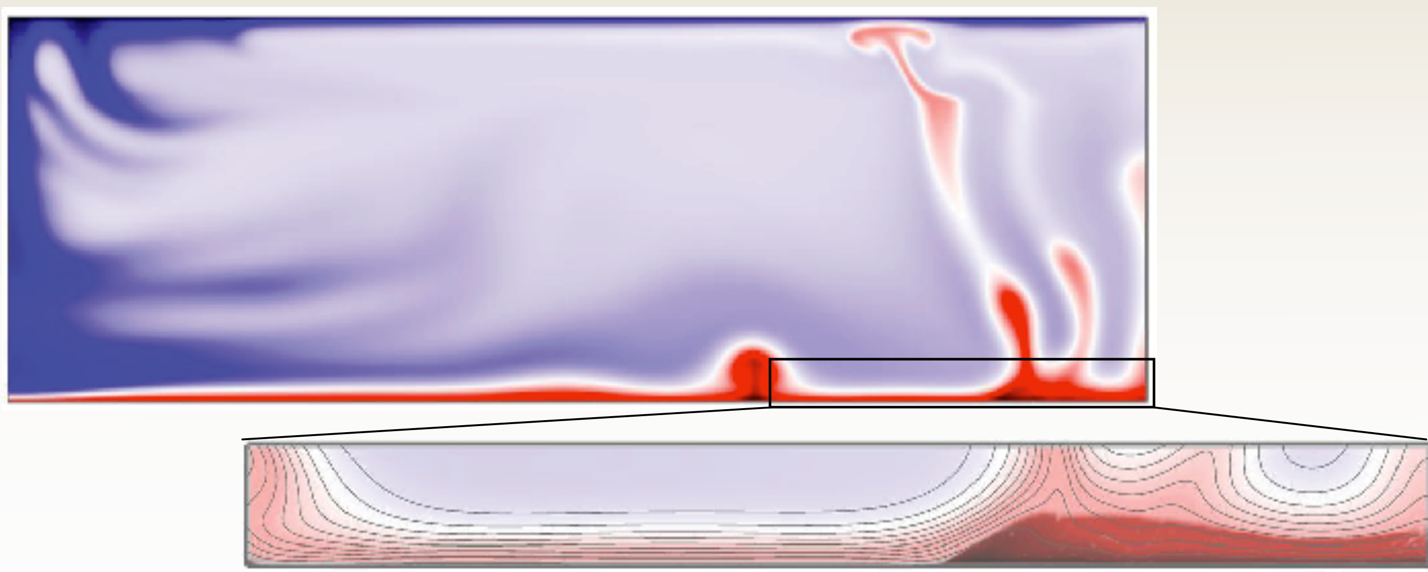

Using CitcomS to perform geodynamical modeling of primordial thermochemical piles and plume clusters using geologic plate history (e.g., Bunge et al., 1998; Lithgow-Bertelloni and Richards, 1998)

Advantages

- Plate motions guide the historical location of subduction, providing an artificial means to impose large wavelength flow
- Allows us to use the spatial information in observations

Disadvantages

- Care must be taken to minimize the momentum violation of kinematic BC's
- Plate history goes back only ~100-150 Myrs, making initial condition an issue

Thermochemical Piles resulting from plate history for past 119 Myrs (starting with a 1D profile).

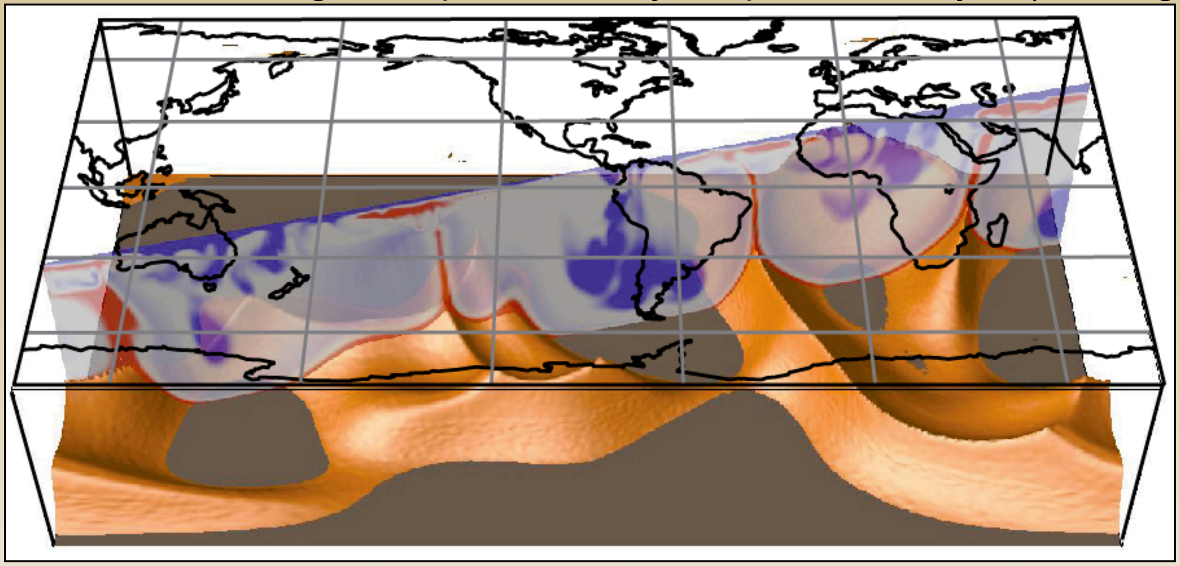

Plume Clusters resulting from plate history for past 119 Myrs (starting with a 1D profile).

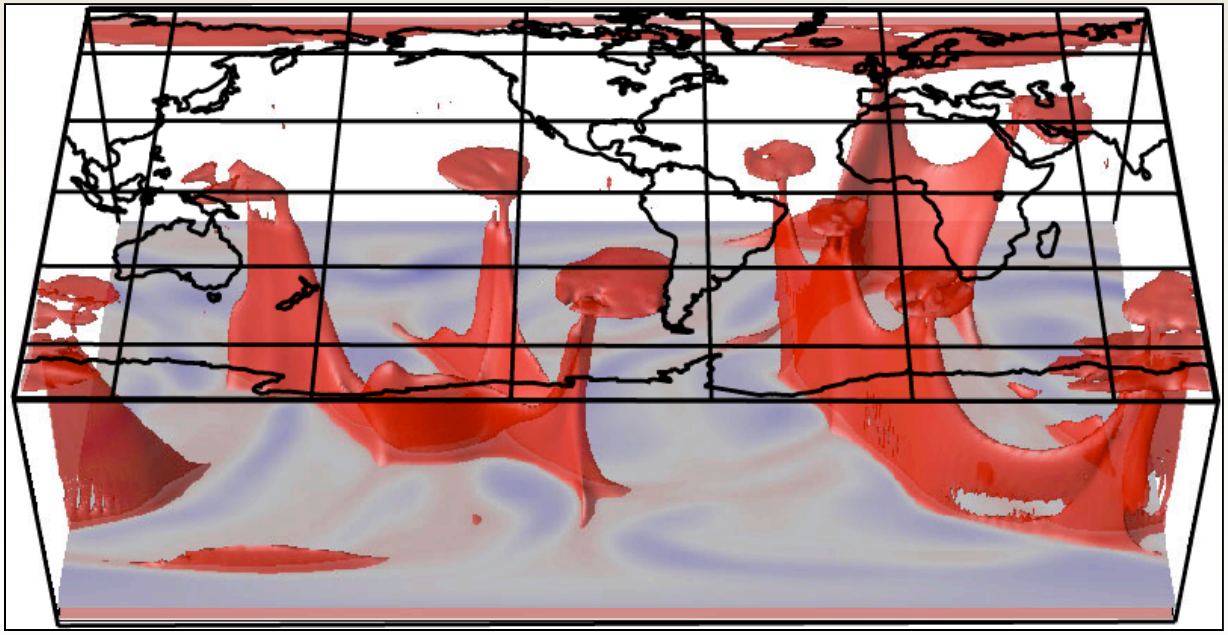

Comparing geodynamical models to seismic tomography.

Work by ASU PhD student, **Abigail Bull** in collaboration with Ritsema, Lithgow-Bertelloni, and Stixrude.

Plume clusters

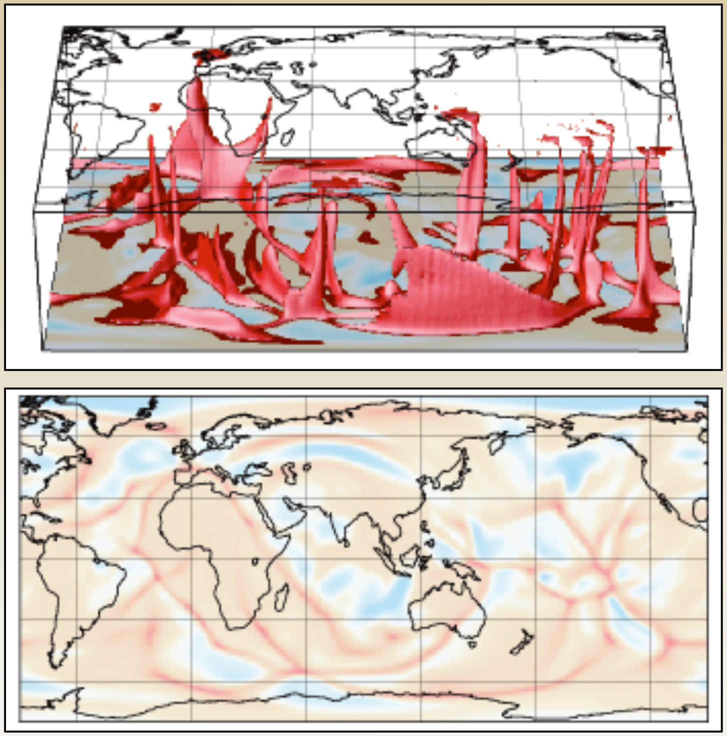

Thermochemical piles

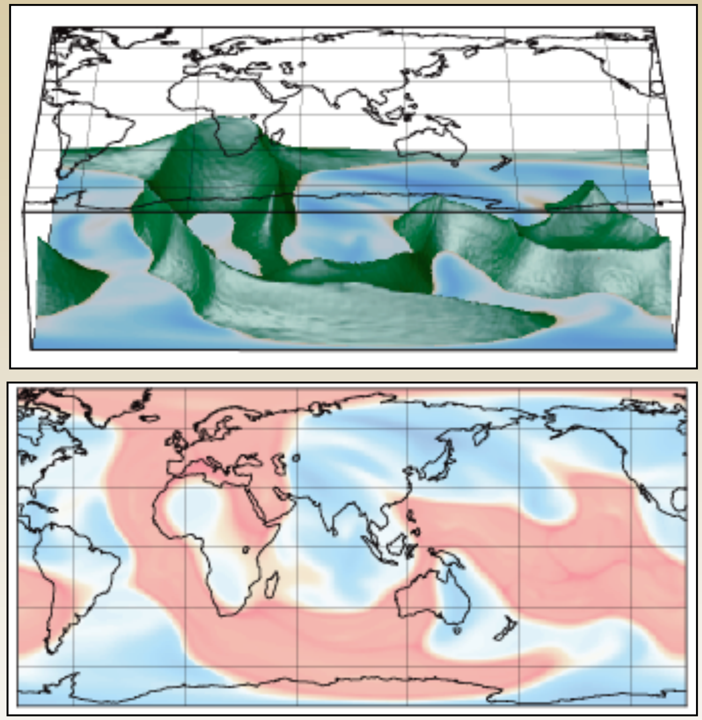

Temperature near CMB

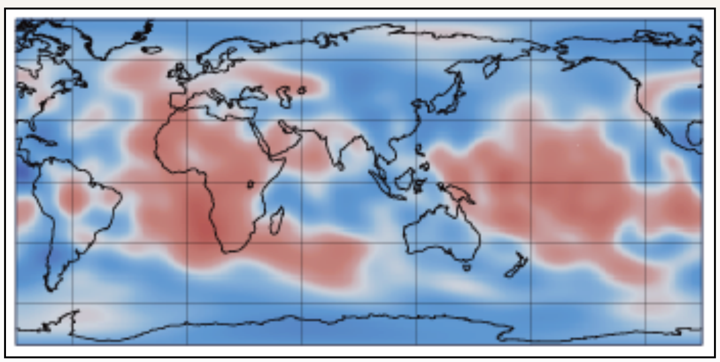

S20RTS

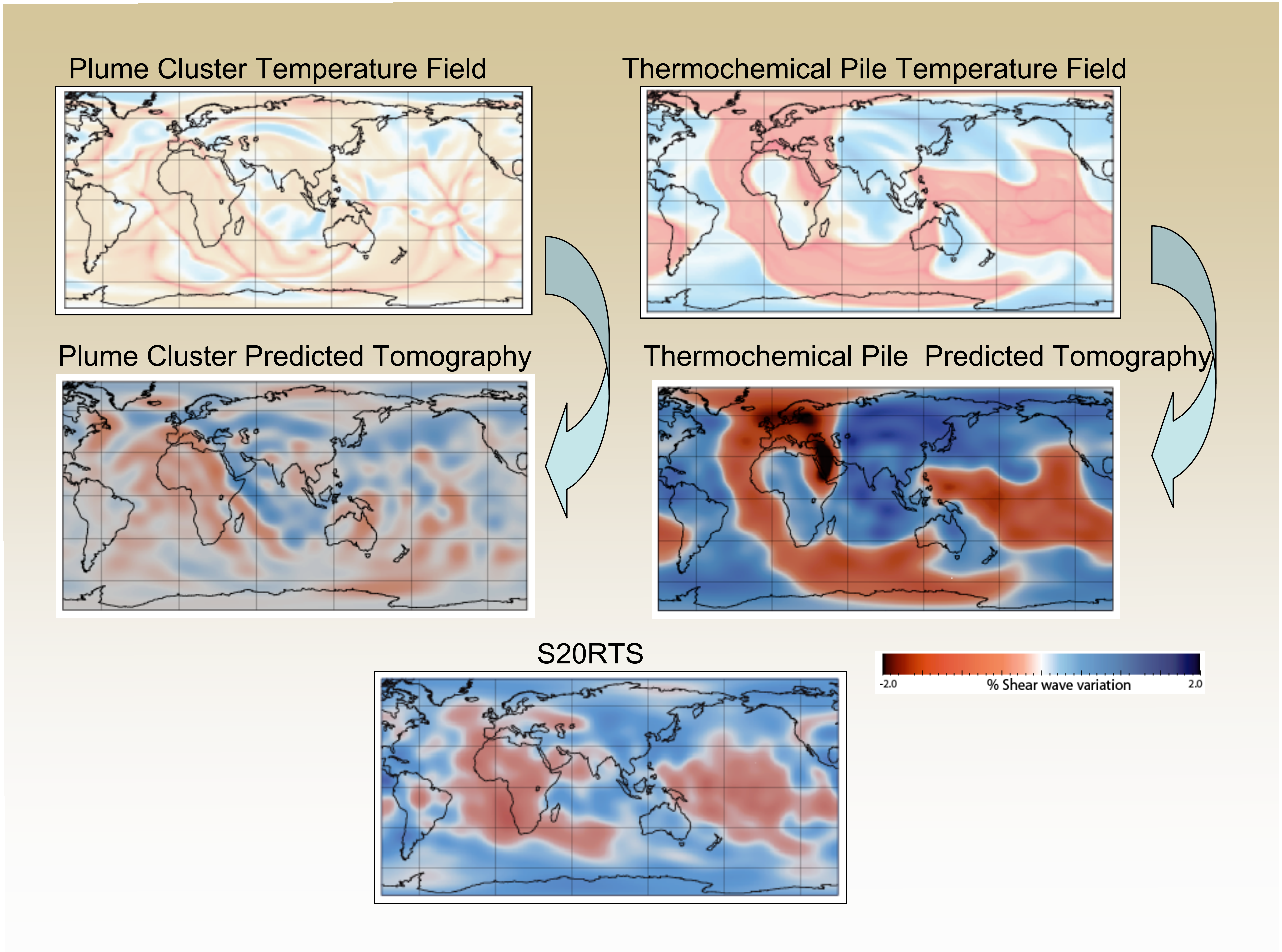
Plume Cluster Temperature Field
Thermochemical Pile Temperature Field
Plume Cluster Predicted Tomography
Thermochemical Pile Predicted Tomography
S20RTS
-2.0
% Shear wave variation
2.0

Plume clusters

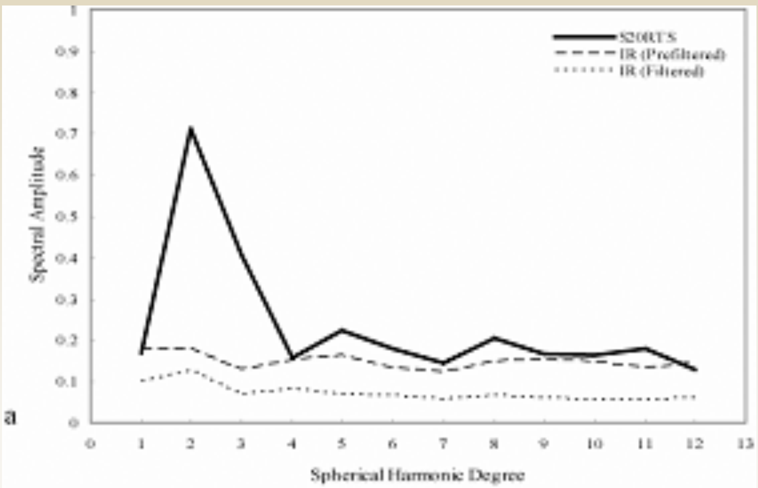

Thermochemical piles

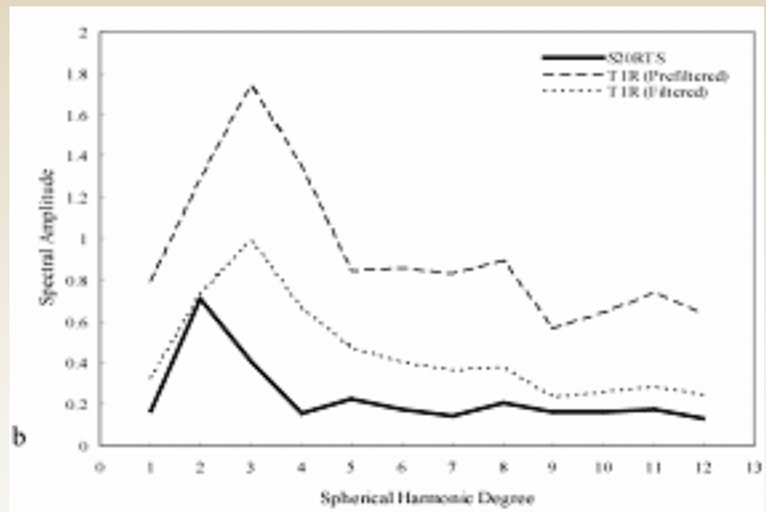

Investigating if dVs/dC is of opposite sign to dVs/dT in thermochemical piles

(i.e., at same P-T, intrinsic wave-speed is faster in pile material than in background material)

Predicted Tomography

0%

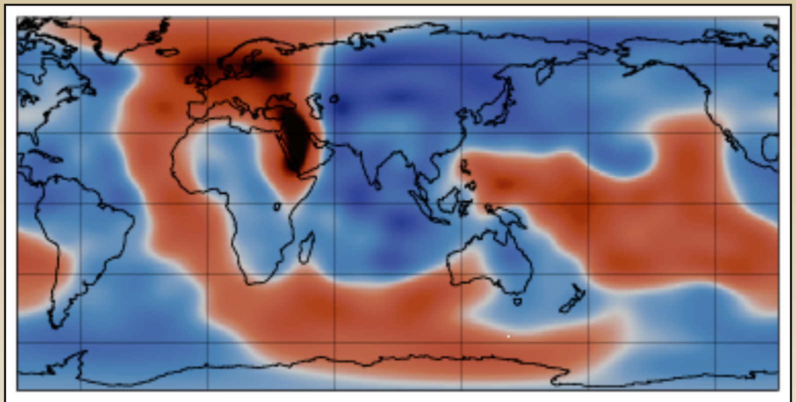

3%

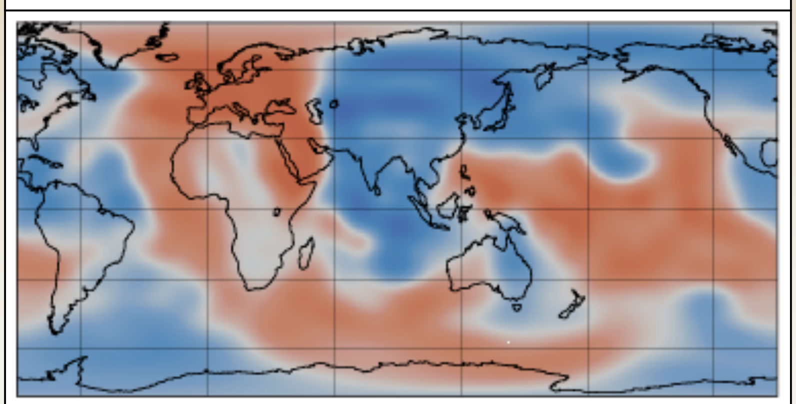

4%

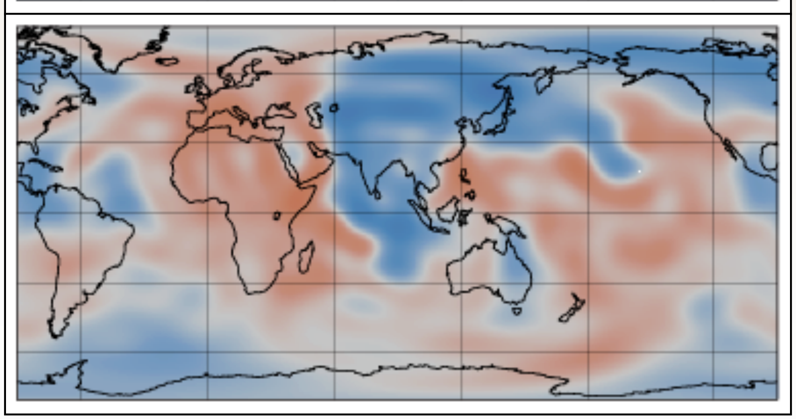

Tomo Model S20RTS

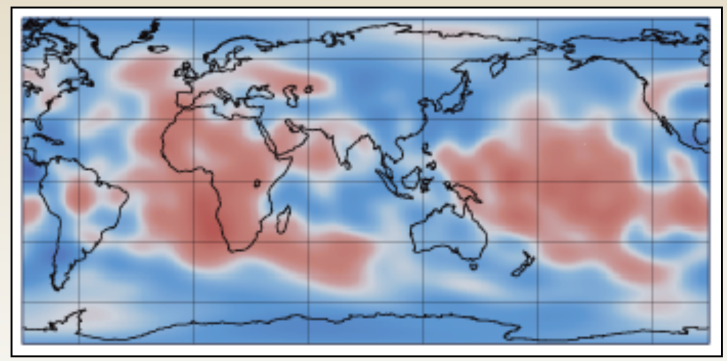

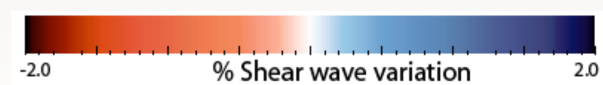

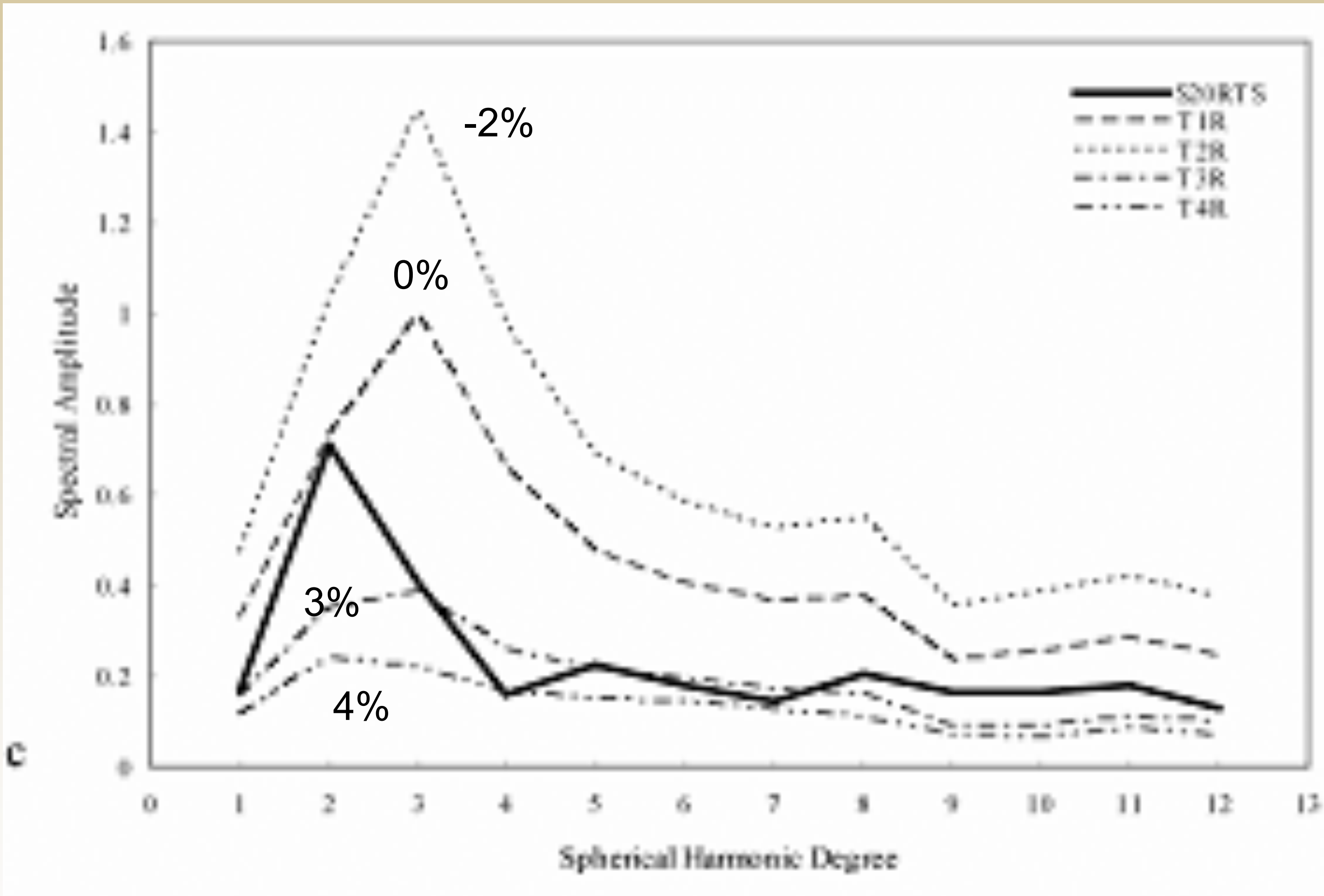

-2%
0%
3%
4%
S20RTS
T1R
T2R
T3R
T4R
Spectral Amplitude
Spherical Harmonic Degree
c

Investigating CMB Temperature (previous calculations done with CMB T of 4000 K)

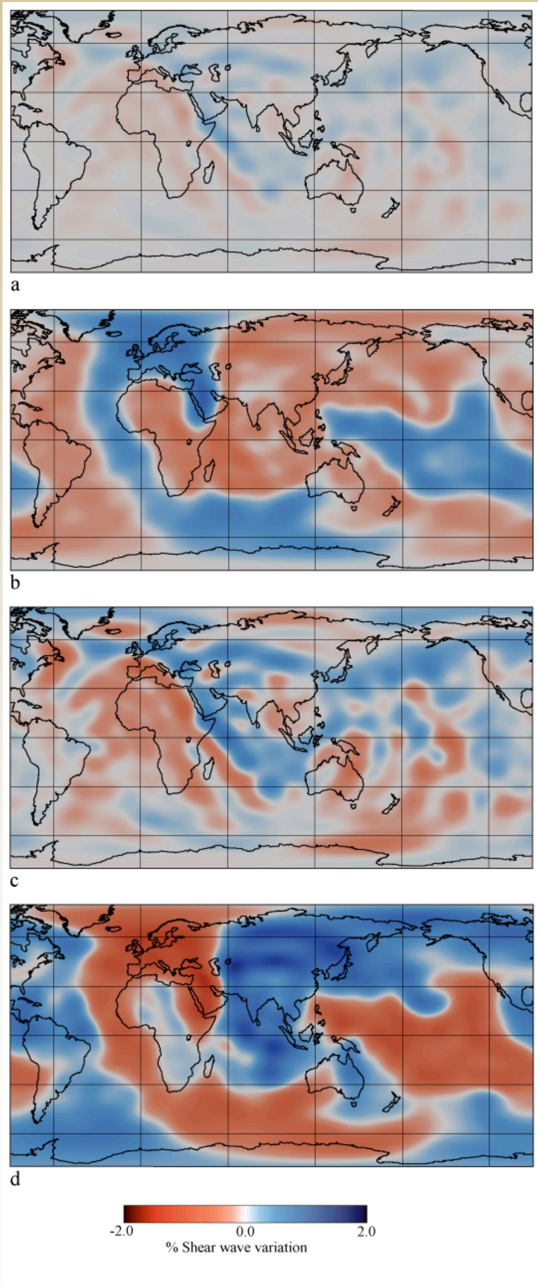

Plume Clusters: CMB 3000 K

Piles (2%): CMB 3000 K

Plume Clusters: CMB 4800 K

Piles (2%): CMB 4800 K

General Findings:

A degree-by-degree statistical correlation shows that both plume clusters and thermochemical piles fit tomography equally well (or perhaps, equally not as well?)

Thermochemical piles reproduce the long-wavelength nature of the power spectrum better than plume clusters as long as they are not composed of material that has a significantly higher shear modulus than background mantle.

Predicted tomography of geodynamic models is very sensitive to assumed CMB temperature. It doesn't matter how well the min phys is known, it is CMB temperature which provides the greatest degree of uncertainty.

Can we use observations of CMB topography as a constraint on the style of thermochemical convection? First step, understand how thermochemical convection affects CMB topography.

Work by ASU graduate student, **Teresa Lassak**.

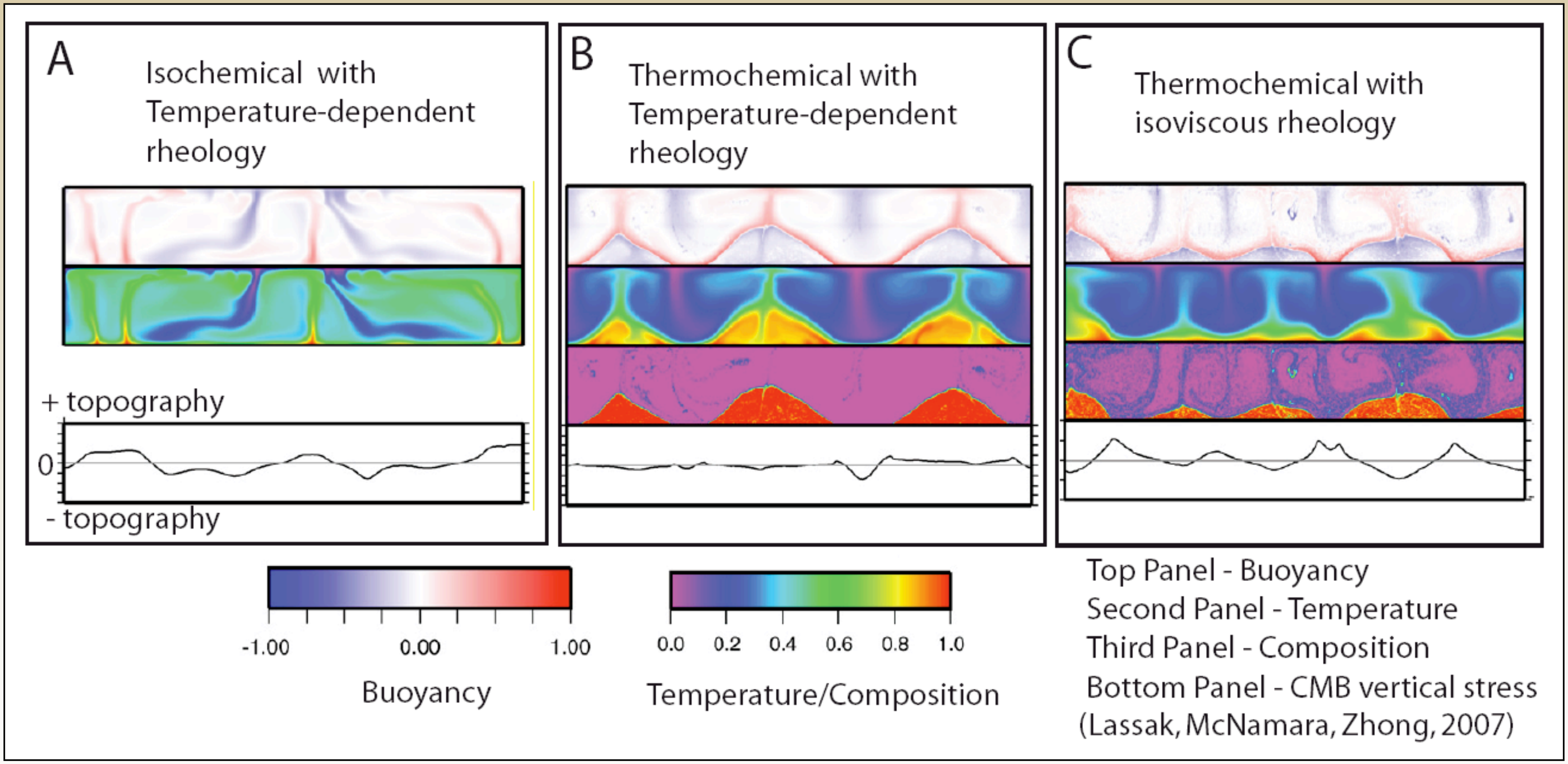

- Temperature-dependence is important.
- In isochemical models, plumes and slabs cause positive and negative CMB topography, respectively
- In thermochemical piles with T-dep. rheology, CMB topo under piles is flat and slightly positive

Plume clusters (temperature-dependent rheology) | Thermochemical Piles (temperature-dependent rheology) | Thermochemical Piles (isoviscous rheology)

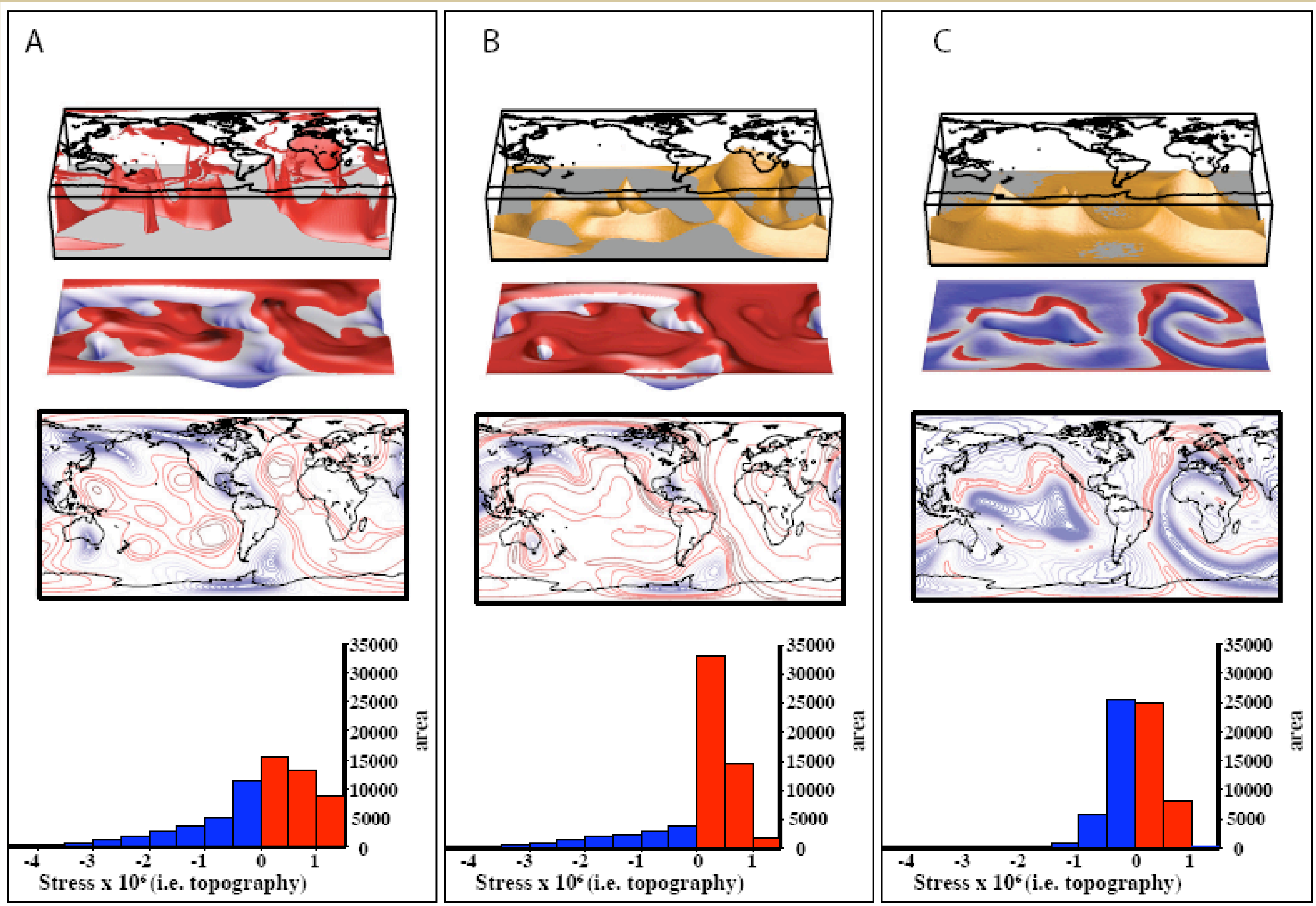

CMB Stress

Results support 2D study

Hypothesis: the style of thermochemical convection causes a unique area distribution of CMB stress.